Jagiellonian University in Kraków

Faculty of Physics, Astronomy and Applied Computer Science

Patryk Kubiczek

Student's book number: 1120897

Spin-triplet pairing in orbitally degenerate Anderson lattice model

Master's Thesis
Field of study: Theoretical Physics

The thesis written under the supervision of
prof. dr hab. Józef Spałek
Department of Condensed Matter Theory and Nanophysics
Marian Smoluchowski Institute of Physics

Kraków 2016

Oświadczenie autora pracy

Świadom odpowiedzialności prawnej oświadczam, że niniejsza praca dyplomowa została napisana przeze mnie samodzielnie i nie zawiera treści uzyskanych w sposób niezgodny z obowiązującymi przepisami.

Oświadczam również, że przedstawiona praca nie była wcześniej przedmiotem procedur związanych z uzyskaniem tytułu zawodowego w wyższej uczelni.

Kraków, dnia Podpis autora pracy

Oświadczenie kierującego pracą

Potwierdzam, że niniejsza praca została przygotowana pod moim kierunkiem i kwalifikuje się do przedstawienia jej w postępowaniu o nadanie tytułu zawodowego.

Kraków, dnia Podpis kierującego pracą

Abstract

This thesis is dedicated to the investigation of a possible theory for uranium-based heavy-fermion ferromagnetic superconductors, stemming from the idea of spin-triplet pairing induced by Hund's rule exchange interaction. For this purpose, we look for approximate solutions of the orbitally-degenerate Anderson lattice model, supplemented with full intra- and inter-orbital Coulombic interactions, which admit non-vanishing equal-spin pairing amplitudes. The approximation scheme we use is the multi-band Gutzwiller method, within which observables evaluation for the variational ground-state is exact in the limit of infinite spatial dimensions. We also compare the results of this method to Hartree-Fock solutions, pointing out the essential role of electronic correlations, which are missing in the latter. In a certain region of model parameters and away from half-filling of electronic bands we find stable spin-triplet superconducting phases, coexistent with ferromagnetic order. Nevertheless, the theory still needs further development in order to make a quantitative comparison to experiment possible.

Keywords: orbitally degenerate Anderson lattice model, ferromagnetic superconductors, Gutzwiller approximation, local spin-triplet pairing, strongly correlated electrons

Abstrakt

Niniejsza praca poświęcona jest badaniom nad możliwą teorią uranowych nadprzewodników ferromagnetycznych, która jest oparta na koncepcji parowania trypletowego indukowanego oddziaływaniem wymiennym Hunda. W tym celu, poszukujemy przybliżonych rozwiązań orbitalnie zdegenerowanego modelu sieci Andersona, rozszerzonego o pełny wewnątrz- i międzyorbitalny hamiltonian oddziaływań kulombowskich, które charakteryzowałyby się nieznikającą amplitudą parowania elektronów o tych samych spinach. Wykorzystaną metodą jest wielopasmowe przybliżenie Gutzwillera, które pozwala na ścisłe obliczanie obserwabli dla wariacyjnego stanu podstawowego w granicy nieskończonego przestrzennego wymiaru. Ponadto porównujemy wyniki tego podejścia z rozwiązaniami w przybliżeniu Hartree-Focka, podkreślając istotną rolę korelacji elektronowych, które nie są w tej drugiej metodzie uwzględniane. Dla pewnego zakresu parametrów modelu, dla mniejszego niż połowiczne wypełnienia pasm elektronowych, obserwujemy stabilne rozwiązanie nadprzewodzące, współistniejące z uporządkowaniem ferromagnetycznym. Niemniej jednak rozważany model wymaga dalszej analizy, by móc ilościowo porównać jego przewidywania z konkretnymi wynikami eksperymentalnymi.

Słowa kluczowe: orbitalnie zdegenerowany model sieci Andersona, nadprzewodniki ferromagnetyczne, przybliżenie Gutzwillera, lokalne parowanie trypletowe, silnie skorelowane elektrony

Acknowledgements

First of all, I would like to give my warmest thanks to Prof. Józef Spałek, who having been my scientific advisor for the last two years, proposed and supervised this thesis. Had it not been for his enthusiasm and commitment, I would not have achieved so much at this stage of my academic path.

I also express my gratitude to the whole Department of Condensed Matter Theory and Nanophysics. It has been a pleasure to work and spend time in this great team. My special thanks must go to Dr. Michał Zegrodnik and Marcin Abram, whose insightful comments helped me prepare this thesis, and to Dr. Danuta Goc-Jagło for her invaluable assistance in formal matters.

Last but not least, I would like to thank my parents and grandparents for their relentless support and confidence in my career decisions. Also, my thanks go to Marta for her understanding and unfailing willingness to discuss the progress of my work.

Funding. The financial support from the Foundation for Polish Science (FNP) within project TEAM (2011-2015) and from the National Science Centre (NCN) under the project MAESTRO, Grant No. DEC-2012/04/A/ST3/00342, are gratefully acknowledged.

Contents

List of Symbols

i, j, k	lattice site index
σ, σ'	spin index
l, l'	orbital index
α, β, γ	electron flavour (combined spin σ and orbital l index)
$\hat{f}^\dagger_{i\alpha}$	= $\hat{f}^\dagger_{il\sigma}$, creation operator of a *correlated* f-electron
$\hat{c}^\dagger_{i\alpha}$	= $\hat{c}^\dagger_{il\sigma}$, creation operator of an *uncorrelated* c-electron
$\hat{n}^f_{i\alpha}$	= $\hat{f}^\dagger_{i\alpha}\hat{f}_{i\alpha}$, number operator of f-electron
$\hat{n}^c_{i\alpha}$	= $\hat{c}^\dagger_{i\alpha}\hat{c}_{i\alpha}$, number operator of c-electron
$\|\Psi_0\rangle$	single-particle product wave-function
$\|\Psi_G\rangle$	variational Gutzwiller wave-function
$\langle\ldots\rangle_0$	= $\langle\Psi_0\|\ldots\|\Psi_0\rangle$, expectation value in the *uncorrelated* $\|\Psi_0\rangle$ state
$\langle\ldots\rangle$	= $\langle\Psi_G\|\ldots\|\Psi_G\rangle$, expectation value in the *correlated* $\|\Psi_G\rangle$ state
$\hat{P}_i$	Gutzwiller variational operator for site i, $\|\Psi_G\rangle = \prod_i \hat{P}_i \|\Psi_0\rangle$
$\|I, i\rangle$	atomic state I of local f-basis at site i
λ	matrix representation of $\hat{P}_i$, $\hat{P}_i = \sum_{II'} \lambda_{II'} \|I, i\rangle\langle I', i\|$
η	Lagrange multipliers corresponding to constraints on λ
ρ	single-particle density matrix, $[\rho_{ij}]^{ab}_{\alpha\beta} = \langle a^\dagger_{i\alpha} b_{i\beta}\rangle_0$
μ	chemical potential
n_f	= $\sum_\sigma \langle\hat{n}^f_{il\sigma}\rangle$, f-electron filling per orbital and per lattice site
n_c	= $\sum_\sigma \langle\hat{n}^c_{il\sigma}\rangle$, c-electron filling per orbital and per lattice site
n	= $\sum_\alpha(\langle\hat{n}^f_{i\alpha}\rangle + \langle\hat{n}^c_{i\alpha}\rangle)$, total electron filling per lattice site
m_f	= $\frac{1}{2}\sum_l(\langle\hat{n}^f_{il\uparrow}\rangle - \langle\hat{n}^f_{il\downarrow}\rangle)$, f magnetic moment per lattice site
m_c	= $\frac{1}{2}\sum_l(\langle\hat{n}^c_{il\uparrow}\rangle - \langle\hat{n}^c_{il\downarrow}\rangle)$, c magnetic moment per lattice site
m	= $m_f + m_c$, total magnetic moment per site
$A_{f\sigma}$	= $\langle\hat{f}^\dagger_{i1\sigma}\hat{f}^\dagger_{i2\sigma}\rangle$, local spin-triplet f pairing amplitude
N	number of lattice sites
E_G	= $\langle\hat{H}\rangle / N$, ground state energy per site
ΔE	= $E_\mathrm{G}(\mathrm{FMSC}) - E_\mathrm{G}(\mathrm{FM})$, condensation energy
$\mathbf{k}$	electronic momentum vector
W	= 1, width of conduction (c) band, unit of energy

Chapter 1

Introduction

The discoveries of ferromagnetic superconductors UGe_2, URhGe, UCoGe, which took place in the previous decade [1–5], led to a renewed interest among physicists in the development of a theory of compatible superconducting and ferromagnetic orders. The superconductivity in the aforementioned actinide heavy-fermion compounds is believed to originate from the same electrons that are responsible for presumably itinerant ferromagnetism. Thus, magnetism and superconductivity do not really compete with each other in those materials, but rather arise from a single physical mechanism. This is in contrast to the case of previously known ferromagnetic superconductors $HoMo_6S_8$ and $ErRh_4B_4$ [6], in which both orders are not homogeneously coexisting, but rather avoid each other by forming a spatially modulated pattern.

It has been argued that ferromagnetic superconductivity has to be of the spin-triplet type, so that the molecular magnetic fields do not lead to breaking of the equal-spin electronic Cooper pairs [7]. Most theoretical works up to date consider p-wave spin-triplet pairing in $\mathbf{k}$-space, as the lowest angular momentum channel ensuring the antisymmetry of the superconducting gap function [8–11]. However, the magnetism, even in its ferromagnetic form, arises from the local spin polarization. Therefore, the natural question may arise whether the pairing can originate also on a local scale and from the same physical source.

In this thesis we discuss an alternative model of spin-triplet superconductivity, which is induced by the intra-atomic Hund's rule interactions among degenerate, correlated and originally atomic f-electrons, which hybridize with a band of conduction electrons and thus form itinerant, perhaps heavy, quasiparticles. In other words, we investigate the possible superconducting solutions of the orbitally degenerate Anderson lattice model, also known by the name of the periodic Anderson model, supplemented with full intra- and inter-orbital Coulombic interactions. The assumed inter-orbital character of the pairing allows us then to consider the simplest case of s-wave pairing, as the pair wave-function is antisymmetric with respect to exchange of the orbital indices. Such a type of pairing has been previously analysed for multi-band Hubbard model [12–19]. However, no phases of coexisting ferromagnetism and superconductivity have been found to be stable, beyond the Hartree-Fock approximation.

The motivation for this work comes from the recent analysis of magnetic phases of uranium digermanide (UGe_2), cf. Fig 1.1, within an orbitally non-degenerate Anderson lattice model [20–22]. In the pressure-temperature phase diagram of UGe_2, shown in Fig. 1.2a, one observes two ferromagnetic phases, separated at low temperatures by a first order transition, as well as a superconducting region located deeply inside those two phases [1, 23]. The most important feature, distinguishing both magnetic phases is the value of uniform magnetic moment they exhibit (Fig. 1.2b): the strongly and weakly saturated phase are

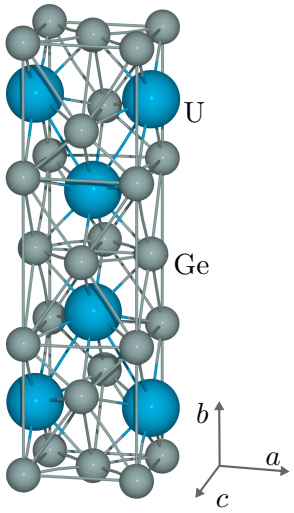

Figure 1.1: Primitive cell of UGe_2, $(a, b, c) = (0.40, 1.51, 0.41)\,\mathrm{nm}$ [25]. UGe_2 crystallizes into orthorhombic centrosymmetric structure and exhibits spontaneous magnetization along a-axis.

called FM2 and FM1, respectively. The critical temperature for superconductivity is very low and reaches its maximum $T_c = 1$ K in the close neighbourhood of the transition point between the ferromagnetic phases at pressure $p = 1.2$ GPa. When pressure is increased further, both superconductivity and ferromagnetism vanish at the same point around $p = 1.6$ GPa, where the material becomes paramagnetic.

In the works [20–22] a two-dimensional character of UGe_2 was assumed. In this thesis we follow the same approach and present results for the model on a square lattice. The justification comes from the band-structure calculation [24], which predicts for this material a quasi-two-dimensional Fermi surface, whose main sheet elongates in b direction of the reciprocal space. Thus, the assumed square lattice is meant to model uranium layers in real space a-c planes, see Fig. 1.1.

Within the orbitally non-degenerate Anderson lattice model the authors of [20–22] were capable of explaining in a semi-quantitative manner the ferromagnetic phases along with classical and quantum critical points appearing in UGe_2 (not all of them are shown in Fig. 1.2). Here, by including the orbital degeneracy, we add a specific mechanism of local spin-triplet pairing based on the Hund's rule intra-atomic and ferromagnetic coupling among the correlated narrow-band electrons, that could possibly explain the nature the of superconducting phase in UGe_2. Nevertheless, our analysis is actually model-oriented and serves only as a starting point for the possible applications to this and other materials.

Our approach is complementary to the discussion of the so-called spin-fluctuation-mediated pairing appearing in its clear form in the limit of weakly correlated electrons [26, 27] but also resulting from strong local electronic correlations [28]. The latter work, which is very recent, is of particular interest to us since it also exploits the idea of inter-orbital spin-triplet pairing due to Hund's exchange. However, it also emphasises the role of local orbital moment fluctuations in the formation of the superconducting gap. In this respect, the concepts contained in [28] constitute a possible idea for continuation of the work presented in this thesis, as we do not take into account any fluctuation within our approximation scheme.

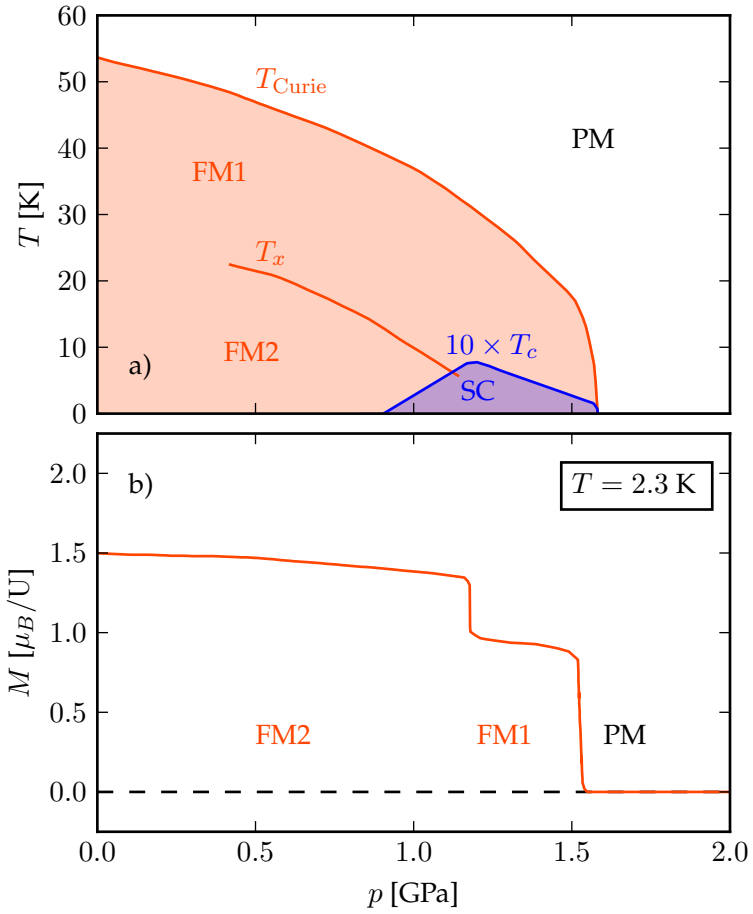

Figure 1.2: a) Schematic pressure p - temperature T phase diagram of UGe_2. b) Magnetization per uranium atom in UGe_2 at temperature $T = 2.3$ K. Both phase transitions are of the first order. Figures adapted from [23].

The method we choose is the Gutzwiller approximation, in the multi-band version developed by Bünemann, Weber and Gebhard [29], which is a variational method allowing for numerically exact evaluation of observables in the infinite dimension limit ($d = \infty$). In a sense, due to special constraints it introduces, it leads to similar results as the statistically-consistent Gutzwiller approximation (SGA), which represents a modified Gutzwiller method, whose standard formulation, also in the case of Anderson lattice model is described in [30–33]. The improvement SGA has introduced is the condition of equality of average electron numbers in the projected and unprojected wave-functions [34, 35]. SGA method turned out to be very successful in describing strongly correlated high-temperature superconductors [36]. It is also Gutzwiller approximation, in the multi-band version, that has been used in the aforementioned analyses of inter-orbital pairing in degenerate Hubbard model [15–19]. Hence, we believe the Gutzwiller method is a good approximation scheme for the model considered in this thesis.

An improved method, namely the diagrammatic expansion for the full

Gutzwiller wave function solution (DE-GWF), which enables one to evaluate observables exactly in any finite dimension d, has been applied to non-degenerate Hubbard and Anderson lattice models [37–40]. However, up to now no extension of this method to a multi-band case has been formulated. Therefore, in this thesis we restrict ourselves only to the zeroth order of the diagrammatic expansion, which is numerically exact only at $d = \infty$.

The thesis is organized as follows. In Chapter 2 we introduce the Hamiltonian of the orbitally degenerate Anderson lattice model and discuss the Hund's rule mechanism of the local spin-triplet pairing. In Chapter 3 we provide an overview of the multi-band Gutzwiller approximation and formulate it specifically for the model analysed in this thesis. In Chapter 4 we present the results obtained for a selected set of model parameters and summarize our present work. The Reader interested in the details of numerical calculations can benefit from reading Appendix A, where we elaborate on our implementation of the multi-band Gutzwiller approximation solver. In Appendix B we explicitly solve the constraints equations and derive the band-narrowing renormalization factors for a non-degenerate Anderson lattice model, to enforce the Reader's intuition concerning the essence of the Gutzwiller approximation.

Chapter 2

Model

Here we discuss the possible model for spin-triplet heavy-fermion ferromagnetic superconductors, considered in this thesis. First, we introduce a doubly degenerate Anderson lattice model supplemented with the full Slater-Kanamori interaction Hamiltonian. Next, we carry out a general discussion of possible types of spin-triplet pairing, taking into account an orbital degree of freedom. We point out that Hund's rule exchange may serve as a driving force for s-wave orbital-singlet spin-triplet pairing in the considered model.

2.1 Anderson lattice model

A popular effective model for the description of heavy-fermion compounds is Anderson lattice model, which describes the hybridization of initially localized $4f$ or $5f$-electrons with mobile conduction electrons

$$\begin{aligned}\hat{H}_{\mathrm{ALM}} = &\sum_{ij\sigma} t_{ij}\hat{c}^{\dagger}_{i\sigma}\hat{c}_{j\sigma} + \epsilon_f \sum_{i\sigma} \hat{f}^{\dagger}_{i\sigma}\hat{f}_{i\sigma} \\ &+ V\sum_{i\sigma}\left(\hat{f}^{\dagger}_{i\sigma}\hat{c}_{i\sigma} + \hat{c}^{\dagger}_{i\sigma}\hat{f}_{i\sigma}\right) + U\sum_{i}\hat{n}^{f}_{i\uparrow}\hat{n}^{f}_{i\downarrow}. \end{aligned} \tag{2.1}$$

In its non-degenerate version it is a two-band model, admitting a set of uncorrelated c-electrons and a set of correlated f-electrons located at energy ϵ_f. The conduction electrons can move between lattice sites, which is reflected in the hopping integrals t_{ij}, forming a band of width W. The two sets of electron states are mixed by an intra-atomic hybridization term with the coupling constant V. The strong electronic correlation of f-electrons is caused by the on-site Coulomb repulsion U, which decreases the probability of double occupied f-levels. This model explains the origin of large effective masses characterizing charge carriers in heavy-fermion compounds, since the hybridization and on-site correlation effects may lead to a strong enhancement of the density of states at chemical potential [41, 42].

The model can be exactly solved in the limit $U = 0$, in which $\hat{H}_{\mathrm{ALM}}$ is diagonalized in the $\mathbf{k}$-space by a Bogoliubov transformation to hybridized quasiparticle states

$$\hat{d}^{\dagger}_{\mathbf{k}\sigma+} = \cos\theta_{\mathbf{k}}\,\hat{c}^{\dagger}_{\mathbf{k}\sigma} + \sin\theta_{\mathbf{k}}\,\hat{f}^{\dagger}_{\mathbf{k}\sigma}, \tag{2.2}$$

$$\hat{d}^{\dagger}_{\mathbf{k}\sigma-} = -\sin\theta_{\mathbf{k}}\,\hat{c}^{\dagger}_{\mathbf{k}\sigma} + \cos\theta_{\mathbf{k}}\,\hat{f}^{\dagger}_{\mathbf{k}\sigma}, \tag{2.3}$$

$$\theta_{\mathbf{k}} = \frac{1}{2}\arctan\left(\frac{2V}{\epsilon_{\mathbf{k}} - \epsilon_f}\right), \tag{2.4}$$

where $\epsilon_{\mathbf{k}}$ are c-electron energies. The resulting spectrum consists of two quasiparticle subbands separated by a gap, which result from quasiparticle energies

$$\mathcal{E}^{\pm}_{\mathbf{k}} = \frac{1}{2}\left(\epsilon_{\mathbf{k}} + \epsilon_f\right) \pm \operatorname{sgn}\left(\epsilon_{\mathbf{k}} - \epsilon_f\right) \frac{1}{2}\sqrt{(\epsilon_{\mathbf{k}} - \epsilon_f)^2 + 4|V|^2}. \tag{2.5}$$

While this solution is valid only in the uncorrelated limit, the intuition gained with its help turns out to be useful in the subsequent analysis, as the correlation effects within Gutzwiller approximation are reflected mostly in a mere renormalization of the strength of hybridization parameter V and a splitting of the location of f-level for up and down spin states.

Nonetheless, the non-degenerate Anderson lattice model is not sufficient for a discussion of possible effects due to inter-orbital interactions between multiple f-states, which may be encountered in real materials, such as the postulated s-wave spin-triplet inter-orbital superconductivity. Therefore we consider an extended Anderson lattice model in which both the c-states of the conduction band and f-electron states possess double orbital degeneracy and are characterized by the orbital index $l = 1, 2$. The full Hamiltonian of such a degenerate model, in which we take into account inter-orbital interactions, splits into several parts

$$\hat{H} = \hat{H}_c + \hat{H}_{fc} + \hat{H}_f + \hat{H}_{\mathrm{int}}, \tag{2.6}$$

$$\hat{H}_c = \sum_{ijl\sigma} t_{ij} \hat{c}^{\dagger}_{il\sigma} \hat{c}_{jl\sigma}, \tag{2.7}$$

$$\hat{H}_{fc} = V \sum_{il\sigma} \left(\hat{f}^{\dagger}_{il\sigma} \hat{c}_{il\sigma} + \hat{c}^{\dagger}_{il\sigma} \hat{f}_{il\sigma} \right), \tag{2.8}$$

$$\hat{H}_f = \epsilon_f \sum_{il\sigma} \hat{f}^{\dagger}_{il\sigma} \hat{f}_{il\sigma}, \tag{2.9}$$

$$\hat{H}_{\mathrm{int}} = \hat{H}_U + \hat{H}_{U'} + \hat{H}_J + \hat{H}_{J'}, \tag{2.10}$$

$$\hat{H}_U = U \sum_{il} \hat{n}^f_{il\uparrow} \hat{n}^f_{il\downarrow}, \tag{2.11}$$

$$\hat{H}_{U'} = \frac{1}{2} U' \sum_{i,\sigma\sigma',l\neq l'} \hat{n}^f_{il\sigma} \hat{n}^f_{il'\sigma'}, \tag{2.12}$$

$$\hat{H}_J = J \sum_{i,l\neq l'} \left(\hat{\mathbf{S}}^f_{il} \hat{\mathbf{S}}^f_{il'} + \frac{1}{4} \sum_{\sigma\sigma'} \hat{n}^f_{il\sigma} \hat{n}^f_{il'\sigma'} \right), \tag{2.13}$$

$$\hat{H}_{J'} = J' \sum_{i,l\neq l'} \hat{f}^{\dagger}_{il\uparrow} \hat{f}^{\dagger}_{il\downarrow} \hat{f}_{il'\downarrow} \hat{f}_{il'\uparrow}, \tag{2.14}$$

where the spin operator $\hat{\mathbf{S}}^f_{il}$ for f-orbitals in the fermionic representation reads

$$\hat{\mathbf{S}}^f_{il} \equiv \hat{f}^{\dagger}_{il\sigma} \frac{\boldsymbol{\sigma}_{\sigma\sigma'}}{2} \hat{f}_{il\sigma'}, \tag{2.15}$$

and $\boldsymbol{\sigma}$ is the vector of Pauli matrices.

The single-particle part of the Hamiltonian: $\hat{H}_c + \hat{H}_{cf} + \hat{H}_f$ and the Hubbard interaction term $\hat{H}_U$ come from the original Anderson lattice model and are tagged by an additional orbital index $l = 1, 2$, which should be understood as a label of a band and not as an orbital quantum number. We do not prescribe

any particular geometrical features to orbital degrees of freedom and assume the full rotational invariance of $\hat{H}$ in the orbital basis.

The remaining part of the interaction Hamiltonian $\hat{H}_{U'} + \hat{H}_J + \hat{H}_{J'}$, originating from Kanamori Hamiltonian [43], describe the inter-orbital interactions. The term $\hat{H}_J$ is of particular significance since it is responsible for the Hund's rule, favouring maximally spin-polarized electronic configurations. The influence of $\hat{H}_{U'}$ on the ground state will be similar as that of $\hat{H}_U$, though it may also result in an orbital-symmetry broken state, the case which we actually do not analyse. The pair-hopping term $\hat{H}'_J$, vanishing within the usual Hartree-Fock mean-field treatment, will probably be of least importance, nevertheless we keep it here to preserve the orbital invariance of $\hat{H}$.

Since the complexity of the model is already quite high, we neglected inter-site interaction terms. We presume that their order of magnitude is much smaller than that of the intra-site interactions. Nevertheless, they still can have an important impact on the physics of real materials, such as Ruderman-Kittel-Kasuya-Yosida (RKKY) interaction, which can trigger a ferro- or anti-ferromagnetic ordering of electronic spins.

As an energy unit we use the width of conduction band $W = 1$ which originates from the hopping integrals t_{ij}. Because t_{ij} is the only non-local integral of the model (i.e. in the momentum space only $\hat{H}_c$ will consist of $\mathbf{k}$-dependent terms), we introduce the lattice geometry via a properly chosen density of states and not via individual t_{ij}. For the details see Appendix A.

Hence, besides the density of states, the model is parametrized by 7 quantities:

- ϵ_f - the shift of f-level with respect to the centre of the conduction band,
- V - hybridization energy of localized f and itinerant c-electrons,
- U - intra-orbital local Coulombic repulsion energy,
- U' - inter-orbital local Coulombic repulsion energy,
- J - Hund's coupling (exchange integral),
- J' - spin-singlet pair hopping energy.

However, two of them are not independent. Assuming Wannier wave-functions of f-electrons are real, we have

$$J' = J. \tag{2.16}$$

Moreover, the following relation results from the full rotational invariance of the orbital basis

$$U' = U - 2J. \tag{2.17}$$

Because the space of model parameters is still quite large, we will be able to analyse only its small but carefully chosen fraction. We discuss the choice of model parameters at the beginning of Chapter 4.

2.2 Spin-triplet pairing

2.2.1 Symmetry properties of the gap function

The interesting question we ask is whether the model defined by the Hamiltonian (2.6) admits superconducting solutions. Such solutions can be characterized by the gap function $\Delta^{ll'}_{\sigma\sigma'}(\mathbf{k})$, whose independent components (up to normalization factors) constitute a set of basis wave-functions for Cooper pairs of relative momentum $\mathbf{k}$ present in the system. Since the gap function has a fermionic

character, it needs to possess the antisymmetry property

$$\Delta^{ll'}_{\sigma\sigma'}(\mathbf{k}) = -\Delta^{l'l}_{\sigma'\sigma}(-\mathbf{k}) \tag{2.18}$$

In BCS theory there is only one band ($l = l'$) and the gap is constant as a function of $\mathbf{k}$ (s-wave pairing) in the neighbourhood of Fermi surface. Thus, the antisymmetry comes from the spin index exchange, indicating that Cooper pairs are in spin-singlet state. In most of theoretical approaches an extension to spin-triplet pairing is achieved by consideration of odd relative angular momentum states, e.g. p-wave, which are antisymmetric in $\mathbf{k}$-space.

In our case, the additional orbital index $l \in \{1, 2\}$ opens the possibility for spin-triplet pairing in s-wave channel, provided the gap is antisymmetric with respect to orbital indices, i.e. it represents an orbital singlet. Then the gap function, treated as a matrix in spin space, acquires the following form

$$\Delta^{ll'}(\mathbf{k}) = \begin{pmatrix} \Delta^{ll'}_{\uparrow\uparrow} & \Delta^{ll'}_{\uparrow\downarrow} \\ \Delta^{ll'}_{\uparrow\downarrow} & \Delta^{ll'}_{\downarrow\downarrow} \end{pmatrix}, \tag{2.19}$$

and is determined by three independent functions $\Delta^{ll'}_{\uparrow\uparrow}$, $\Delta^{ll'}_{\uparrow\downarrow}$, $\Delta^{ll'}_{\downarrow\downarrow}$ satisfying condition

$$\Delta^{ll'}_{\sigma\sigma'} = -\Delta^{l'l}_{\sigma\sigma'}. \tag{2.20}$$

2.2.2 Pairing induced by Hund's rule

Here we discuss the mechanism of Hund's rule induced spin-triplet pairing [14], which can be realized in the considered model.

We express the inter-orbital part of the Hamiltonian $\hat{H}_{U'} + \hat{H}_J$ in terms of 'pairing' operators: $\hat{B}^\dagger_{ill'}$ and vector-like $\hat{\mathbf{A}}^\dagger_{ill'm}$

$$H_J + H_{U'} = \frac{1}{2}(U' + J) \sum_{i,l\neq l'} \hat{B}^\dagger_{ill'}\hat{B}_{ill'} + \frac{1}{2}(U' - J) \sum_{i,l\neq l'} \hat{\mathbf{A}}^\dagger_{ill'}\hat{\mathbf{A}}_{ill'}, \tag{2.21}$$

where

$$\hat{B}^\dagger_{ill'} \equiv \frac{1}{\sqrt{2}}\left(\hat{f}^\dagger_{il\uparrow}\hat{f}^\dagger_{il'\downarrow} - \hat{f}^\dagger_{il\downarrow}\hat{f}^\dagger_{il'\uparrow}\right) \tag{2.22}$$

creates an inter-orbital f-electron pair in spin-singlet channel and

$$\hat{\mathbf{A}}^\dagger_{ill'} \equiv \left(\hat{f}^\dagger_{il\uparrow}\hat{f}^\dagger_{il'\uparrow}, \frac{1}{\sqrt{2}}\left(\hat{f}^\dagger_{il\uparrow}\hat{f}^\dagger_{il'\downarrow} + \hat{f}^\dagger_{il\downarrow}\hat{f}^\dagger_{il'\uparrow}\right), \hat{f}^\dagger_{il\downarrow}\hat{f}^\dagger_{il'\downarrow}\right) \tag{2.23}$$

is a three-component spin triplet pair creating operator. If $J > U'$ this term would provide an attractive interaction between electrons in spin-triplet channel. Therefore, in an analogy to BCS theory, one concludes that it may be energetically favourable for a system to condense into state characterized by anomalous averages

$$\left\langle \hat{\mathbf{A}}_{ill'} \right\rangle \neq 0 \tag{2.24}$$

Note that, unlike in BCS theory, this is a scenario of real-space pairing being purely local, which means that the s-wave gap is uniform in the whole $\mathbf{k}$-space. The nature of this superconducting state differs from the BCS picture and the lone appearance of pairing correlations may be insufficient for the system to become superconducting. It has been postulated that a key ingredient for the

appearance of superconductivity in this case is Bose-Einstein condensation (BEC) of tightly bound local electronic pairs. However, it is believed that those two scenarios of pairing are two facets of the same physical mechanism, which can be continuously connected via so called BEC-BCS crossover [44, 45]. Thus, in the forthcoming we neglect the discussion of the possible Bose-Einstein condensation of spin-triplet Cooper pairs and focus solely on finding the equal-spin pairing amplitudes $\langle \hat{f}^{\dagger}_{i1\uparrow} \hat{f}^{\dagger}_{i2\uparrow} \rangle$ and $\langle \hat{f}^{\dagger}_{i1\downarrow} \hat{f}^{\dagger}_{i2\downarrow} \rangle$ within a BCS-like approach.

Chapter 3

Multi-band Gutzwiller approximation

Here we discuss the multi-band Gutzwiller approximation within which we solve the model. The multi-band Gutzwiller approximation, as introduced by Bünemann, Weber and Gebhard [29], derives originally from the work of Gebhard [46] who reformulated the original Gutzwiller approximation [30] as the $1/d$ expansion, with d being the dimensionality of a system. The inclusion of superconductivity to the multi-band Gutzwiller approximation was later proposed in [47] and was successfully applied to an extended two-band Hubbard model in [16, 18]. The derivation of the method presented here is closest to the one in [48].

3.1 General formulation

3.1.1 Gutzwiller wave-function

The multi-band Gutzwiller approximation is a variational method in which the following trial wave-function is utilised

$$|\Psi_G\rangle = \prod_i \hat{P}_i \, |\Psi_0\rangle \,, \tag{3.1}$$

where $|\Psi_0\rangle$ is a product of single-particle wave-functions (Slater determinant), in general describing non-correlated broken symmetry states, for which Wick's theorem hold. $\hat{P}_i$ is so called "Gutzwiller projector" for site i (though formally it is not a projection operator). The most general form of the operator $\hat{P}_i$ reads

$$\hat{P}_i = \sum_{II'} [\lambda_i]_{II'} \left| I, i \right\rangle\!\!\left\langle I', i \right| , \tag{3.2}$$

where the states $\{|I, i\rangle\}_I$ span the local Fock basis of the correlated orbitals at site i and the matrices λ_i consist of variational parameters. In principle λ_i can be any complex-valued matrix, although for simplicity we restrict ourselves to real-valued symmetric matrices.

Any state $|I, i\rangle$ is fully determined by the set of the occupied spin-orbital states. In the language of second quantization we write

$$|I, i\rangle = \prod_{\alpha \in I}^{<} \hat{f}^\dagger_{i\alpha} \, |0, i\rangle \,, \tag{3.3}$$

where $\alpha = (l, \sigma)$ denotes a combined flavour index, the "$<$" symbol means the creation operators should be ordered with an increasing flavour index α and $|0, i\rangle$ is the unoccupied state at site i.

The operator $|I, i\rangle\langle I', i|$ transforms state $|I', i\rangle$ into $|I, i\rangle$ and reduces to zero while acting on any other state. Within the convention set by (3.3), its second-quantized form is

$$\big|I, i\big\rangle\big\langle I', i\big| = \prod_{\alpha\in I}^{<} \hat{f}^{\dagger}_{i\alpha} \prod_{\beta\in I'}^{>} \hat{f}_{i\beta} \prod_{\gamma\notin I\cup I'} (1 - \hat{n}^{f}_{i\gamma}). \tag{3.4}$$

It should be stressed out that even though we use the same Dirac notation for the full wave-function (3.1) and local states (3.3), these objects belong to different Hilbert spaces. In other words, the operators (3.4) act only in local (i.e. restricted to a given site i) subspaces spanned by the correlated orbitals. A tensor product of those local subspaces and of local subspaces spanned by some uncorrelated orbitals (e.g conduction band in Anderson lattice model), forms the full Hilbert space of the model.

The idea behind the variational wave-function (3.1) is to decrease the probabilities of certain energetically unfavourable electronic configurations such us double occupancies of f-states. The non-diagonal terms of λ_i lead to the mixing of those configurations which occurs for example for spin-flip interactions. In the case of local superconducting pairing it is also necessary to include terms mixing local configurations of different electron number.

3.1.2 Evaluation of observables

The non-trivial part of the multi-band Gutzwiller approximation is the evaluation of observables. Except some special cases in $d = 1$, the exact evaluation is possible only in the limit $d = \infty$, i.e. in the limit of infinite lattice coordination number. This follows from the observation that the contraction of a pair of creation and annihilation operators at sites i and j scales with their taxicab (Manhattan) distance $\|\mathbf{i} - \mathbf{j}\|$ as

$$\left\langle \hat{f}^{\dagger}_{i\alpha} \hat{f}_{j\alpha} \right\rangle \sim \left(\frac{1}{\sqrt{d}} \right)^{\|\mathbf{i}-\mathbf{j}\|}. \tag{3.5}$$

Here we present a heuristic justification of (3.5). The squared modulus of the discussed contraction represents the probability of electron tunnelling from i to j. If we fix i and allow only for the nearest neighbour hopping, the probability should be roughly equally distributed among Z nearest neighbours

$$\left| \left\langle \hat{f}^{\dagger}_{i\alpha} f_{i+1,\alpha} \right\rangle \right|^2 \approx \frac{1}{Z}. \tag{3.6}$$

Assuming the linear scaling of lattice coordination number Z with dimensionality d we obtain the desired result. For formal derivation see [49].

Now, let us consider expectation value of a purely local operator $\hat{O}_i$. Such an operator can always be expressed in terms of local creation and annihilation operators

$$\hat{O}_i = \hat{O}_i\Big(\big\{ \hat{f}^{\dagger}_{i\alpha} \big\}_{\alpha}, \big\{ \hat{f}_{i\alpha} \big\}_{\alpha} \Big). \tag{3.7}$$

Then, if $\hat{P}_i$ are Hermitian, its expectation value is given by

$$\left\langle \Psi_G \middle| \hat{O}_i \middle| \Psi_G \right\rangle = \frac{\left\langle \Psi_0 \middle| \left(\prod_j \hat{P}_j \right) \hat{O}_i \left(\prod_j \hat{P}_j \right) \middle| \Psi_0 \right\rangle}{\left\langle \Psi_0 \middle| \left(\prod_j \hat{P}_j \right) \left(\prod_j \hat{P}_j \right) \middle| \Psi_0 \right\rangle}. \tag{3.8}$$

Let us introduce shorthand notation $\langle \Psi_G | \ldots | \Psi_G \rangle \equiv \langle \ldots \rangle$ and $\langle \Psi_0 | \ldots | \Psi_0 \rangle \equiv \langle \ldots \rangle_0$. Since the operators $\hat{P}_i, \hat{P}_j$ commute for $i \neq j$, equation (3.8) can be rearranged

$$\left\langle \hat{O}_i \right\rangle = \frac{\left\langle \left(\prod_{j \neq i} \hat{P}_j^2 \right) \hat{P}_i \hat{O}_i \hat{P}_i \right\rangle_0}{\left\langle \prod_j \hat{P}_j^2 \right\rangle_0}. \tag{3.9}$$

For a moment let as assume that $|\Psi_G\rangle$ is normalized, so we do not need to write down the denominator. Applying Wick's theorem this expectation value decomposes into the following terms

$$\left\langle \hat{O}_i \right\rangle = \left\langle \prod_{j \neq i} \hat{P}_j^2 \right\rangle_0 \left\langle \hat{P}_i \hat{O}_i \hat{P}_i \right\rangle_0 + \sum_{\substack{\text{all pairs} \\ \text{of n. n.} \\ \text{contractions}}} \left\langle \overbrace{\prod_{j \neq i} \hat{P}_j^2} \right\rangle_0 \left\langle \overbrace{\hat{P}_i \hat{O}_i \hat{P}_i} \right\rangle_0 + \ldots, \tag{3.10}$$

where the symbol

$$\sum_{\substack{\text{all pairs} \\ \text{of n. n.} \\ \text{contractions}}} \left\langle \overbrace{\hat{\mathcal{A}}} \right\rangle_0 \left\langle \overbrace{\hat{\mathcal{B}}} \right\rangle_0$$

denotes the following operation:

1. From creation and annihilation operators constituting $\hat{\mathcal{A}}$ choose a single creation (or annihilation) operator $\hat{f}^\dagger_{j\alpha}$ ($\hat{f}_{j\alpha}$).
2. Choose a single annihilation (or creation) operator $\hat{f}^\dagger_{i\alpha}$ ($\hat{f}_{i\alpha}$) from $\hat{\mathcal{B}}$, such that site i is the nearest neighbour of j.
3. Repeat the steps 1. and 2., not choosing again the previously selected operators.
4. Contract, i.e. calculate the expectation values of those two pairs of operators.
5. Contract all the remaining operators within $\hat{\mathcal{A}}$.
6. Contract all the remaining operators within $\hat{\mathcal{B}}$.
7. Multiply all the calculated expectation values altogether.
8. Repeat the procedure above for all the possible choices made in steps 2. and 3., and sum all the resulting terms.

Within this notation, each contraction line brings in a contribution of $1/\sqrt{d}$ coming from nearest neighbour contractions. Further terms in (3.10) will contain more nearest neighbour contractions, or contractions between subsequent neighbours.

Because of (3.5) we presume that the first term of (3.10) will simplify to $\langle \hat{P}_i \hat{O}_i \hat{P}_i \rangle$ in the limit $d = \infty$ if for each site i we apply the constraint

$$\left\langle \hat{P}_i^2 \right\rangle_0 = 1. \tag{3.11}$$

We also presume that this is a sufficient condition for the normalization of the wave-function $|\Psi_G\rangle$. However, as we shall see, (3.11) is not enough, because the

non-local contributions will add up to each other and may still be important. Moreover, one would naively expect that all the other terms in (3.10), in which some operators are contracted non-locally, vanish in the limit $d = \infty$. That is not correct as well.

We limit our discussion to the case where only the flavour-diagonal density matrix elements $\langle \hat{f}^\dagger_{i\alpha} \hat{f}_{j\alpha} \rangle$ are present. This can always be accomplished by a suitable Bogoliubov transformation of the flavour basis. Let us now focus on the sum from equation (3.10). We explain again how each term of this sum is calculated. At first, one chooses a pair of creation and annihilation operators from $\prod_{j \neq i} \hat{P}_j^2$, restricting oneself only to j's being the nearest neighbours of i. Then another pair is chosen from $\hat{P}_i \hat{O}_i \hat{P}_i$ and respective operators are contracted producing a factor $1/d$. Those two non-local contractions have to connect i with the same site j, otherwise there would be a non-local contraction in $\prod_{j \neq i} \hat{P}_j^2$ leading to an additional factor $1/\sqrt{d}$. Finally, the remaining operators are contracted locally. This means that the number of terms in the sum is of order d, so overall the sum does not vanish in the limit $d \to \infty$.

In order to cure this the following constraint is introduced for each flavour α and site i

$$\left\langle \hat{P}_i^2 \hat{f}^\dagger_{i\alpha} \hat{f}_{i\alpha} \right\rangle_0 = \left\langle \hat{f}^\dagger_{i\alpha} \hat{f}_{i\alpha} \right\rangle_0 . \tag{3.12}$$

The left hand side of (3.12) can be rewritten

$$\left\langle \hat{P}_i^2 \hat{f}^\dagger_{i\alpha} \hat{f}_{i\alpha} \right\rangle_0 = \left\langle \hat{P}_i^2 \right\rangle_0 \left\langle \hat{f}^\dagger_{i\alpha} \hat{f}_{i\alpha} \right\rangle_0 + \sum_{\substack{\text{all pairs} \\ \text{of c. and a.} \\ \text{operators}}} \overbrace{\left\langle \hat{P}_i^2 \right\rangle_0 \hat{f}^\dagger_{i\alpha} \hat{f}_{i\alpha}}. \tag{3.13}$$

The last term of (3.13) results from choosing all the possible pairs of $\hat{f}^\dagger_{i\alpha}$ and $\hat{f}_{i\alpha}$ from ${\hat{P}_i}^2$ and contracting each pair element with one of the operators from $\hat{f}^\dagger_{i\alpha} \hat{f}_{i\alpha}$. Because of (3.11) and (3.12) this term vanishes. This has a far-reaching implications when we further analyse the structure of this term

$$\sum_{\substack{\text{all pairs} \\ \text{of c. and a.} \\ \text{operators}}} \overbrace{\left\langle \hat{P}_i^2 \right\rangle_0 \hat{f}^\dagger_{i\alpha} \hat{f}_{i\alpha}} = \left(\sum_{\substack{\text{all pairs} \\ \text{of c. and a.} \\ \text{operators}}} \left\langle \left[\hat{P}_i^2 \right]_{\substack{\text{c. and a.} \\ \text{operators} \\ \text{removed}}} \right\rangle_0 \right) \left\langle \hat{f}^\dagger_{i\alpha} \hat{f}_{i\alpha} \right\rangle_0 = 0, \tag{3.14}$$

where

$$\left[\hat{\mathcal{A}} \right]_{\substack{\text{c. and a.} \\ \text{operators} \\ \text{removed}}}$$

denotes a product operator $\hat{\mathcal{A}}$ from which some creation and annihilation operators are taken away.

Now, since we usually want $\langle \hat{f}^\dagger_{i\alpha} \hat{f}_{i\alpha} \rangle_0 \neq 0$, the pre-factor appearing in (3.14) has to vanish. The crucial observation is that the sum in (3.10) can be grouped into terms of the form

$$\left(\sum_{\substack{\text{all pairs} \\ \text{of c. and a.} \\ \text{operators}}} \left\langle \left[\hat{P}_j^2 \right]_{\substack{\text{c. and a.} \\ \text{operators} \\ \text{removed}}} \right\rangle_0 \right) \left\langle \hat{f}^\dagger_{i\alpha} \hat{f}_{j\alpha} \right\rangle_0 \left\langle \hat{f}^\dagger_{j\alpha} \hat{f}_{i\alpha} \right\rangle_0 \left\langle \left[\hat{P}_i \hat{O}_i \hat{P}_i \right]_{\substack{\text{c. and a.} \\ \text{operators} \\ \text{removed}}} \right\rangle_0 .$$

Therefore, enforcing (3.11) and (3.12) leads to the elimination of all the non-local contributions to the evaluation of local observables in the limit $d = \infty$. Also, it

leads to the desired simplification of the first term in (3.10), which can be easily shown by analogous arguments. Namely

$$\left\langle \hat{O}_i \right\rangle = \left\langle \hat{P}_i \hat{O}_i \hat{P}_i \right\rangle_0 . \tag{3.15}$$

Analogous considerations lead to

$$\left\langle \hat{O}_{ij} \right\rangle = \left\langle \hat{P}_i \hat{P}_j \hat{O}_{ij} \hat{P}_j \hat{P}_i \right\rangle_0 . \tag{3.16}$$

However, in this thesis we never need to evaluate such non-local observables for correlated orbitals.

Taking into account further terms in (3.10) it is possible to construct a proper $1/d$ expansion around $d = \infty$. Nonetheless, the computational complexity, especially for a multi-orbital problem, would grow tremendously if we tried to include even the first order expansion terms. Hence we limit ourselves only to the zeroth order of $1/d$ expansion, which we simply call the (multi-band) Gutzwiller approximation.

It is also worth noting that constraints (3.11) and (3.12) greatly simplify calculation of the expectation values of operators acting only in the space of uncorrelated orbitals. For

$$\hat{O}_c = \hat{O}_c\Big(\{\hat{c}^\dagger_{i\alpha}\}_{i,\alpha}, \{\hat{c}_{i\alpha}\}_{i,\alpha} \Big) \tag{3.17}$$

we have

$$\left\langle \hat{O}_c \right\rangle = \left\langle \Big(\prod_j \hat{P}_j^2 \Big) \hat{O}_c \right\rangle_0 = \left\langle \hat{O}_c \right\rangle_0 \tag{3.18}$$

and all the non-local contributions vanish due to reasons similar to those presented above.

3.1.3 Energy functional minimization

Having a recipe for the evaluation of observables, we can eventually calculate the ground state energy $\langle \hat{H} \rangle$. Now the task is to set up a procedure of finding the matrices λ_i and single-particle wave-function $|\Psi_0\rangle$ which minimize this quantity subject to constraints (3.11) and (3.12). However, it is not practical to treat the whole wave-function $|\Psi_0\rangle$ as a variational object. Instead, we will perform the optimization with respect to the elements of a single particle density matrix ρ, which completely determines $|\Psi_0\rangle$. Namely,

$$[\rho_{ij}]^{ab}_{\alpha\beta} = \left\langle \hat{a}^\dagger_{i\alpha} \hat{b}_{i\beta} \right\rangle_0 , \tag{3.19}$$

where $a, b \in \{f, c\}$ are operators for correlated or uncorrelated orbitals.

When λ_i has non-diagonal elements, it is very cumbersome to solve explicitly the constraints and reduce the number of independent variational parameters. However, in Appendix B we present a case of non-degenerate Anderson lattice model, for which it can actually be done. We encourage the Reader to study this example in order to gain some intuition about the physical ideas behind the Gutzwiller approximation.

Nevertheless, the general method to enforce the constraints is to introduce Lagrange parameters $\eta_i, \eta_{i\alpha}$ and to find the stationary points of the functional

$$L(\rho,\mu,\lambda,\eta) = \left\langle \hat{H} \right\rangle - \mu \sum_i \left(\sum_\alpha \left\langle \hat{n}^f_{i\alpha} \right\rangle + \sum_\beta \left\langle \hat{n}^c_{i\beta} \right\rangle - n \right) + \sum_i \eta_i \left(\left\langle \hat{P}_i^{\,2} \right\rangle_0 - 1 \right) + \sum_{i\alpha} \eta_{i\alpha} \left(\left\langle \hat{P}_i^{\,2} \hat{f}^\dagger_{i\alpha} \hat{f}_{i\alpha} \right\rangle_0 - \left\langle \hat{f}^\dagger_{i\alpha} \hat{f}_{i\alpha} \right\rangle_0 \right), \quad (3.20)$$

which correspond to the aforementioned minima of $\langle \hat{H} \rangle$. The chemical potential μ in (3.20) allows us for keeping the average filling per site n fixed, i.e.

$$n = \frac{1}{N} \sum_i \left(\sum_\alpha \left\langle \hat{n}^f_{i\alpha} \right\rangle + \sum_\beta \left\langle \hat{n}^c_{i\beta} \right\rangle \right) \quad (3.21)$$

Now, we demand that

$$\frac{\partial L(\rho,\mu,\lambda,\eta)}{\partial \left[\lambda_i\right]_{II'}} = 0 \quad (3.22)$$

The minimization with respect to ρ is more involved. We need to supply the functional L with a constraint $\rho^2 = \rho$, which represents both necessary and sufficient conditions for ρ being a proper single-particle density matrix. We create a new functional $\mathcal{L}$ explicitly depending on another set of Lagrange multipliers, grouped into matrix χ

$$\mathcal{L}\left(\rho,\mu,\lambda,\eta,\chi\right) = L - \sum_{ij,ab,\alpha\beta} \left[\chi_{ij}\right]^{ab}_{\alpha\beta} \left(\sum_{k,d,\gamma} \left[\rho_{ik}\right]^{ad}_{\alpha\gamma} \left[\rho_{kj}\right]^{db}_{\gamma\beta} - \left[\rho_{ij}\right]^{ab}_{\alpha\beta} \right) \quad (3.23)$$

The physical equilibrium condition is

$$\frac{\partial \mathcal{L}}{\partial \left[\rho_{ij}\right]^{ab}_{\alpha\beta}} = 0 \quad (3.24)$$

If we define

$$\left[H_{\text{eff}}\right]^{ab}_{ij,\alpha\beta} = \frac{\partial L}{\partial \left[\rho_{ij}\right]^{ab}_{\alpha\beta}} \quad (3.25)$$

then (3.24) leads to a matrix equation

$$H_{\text{eff}} = \chi \cdot \rho + \rho \cdot \chi - \chi \quad (3.26)$$

When $\rho^2 = \rho$, a sufficient condition for the equation (3.26) to be fulfilled is

$$\left[H_{\text{eff}}, \rho\right] = 0 \quad (3.27)$$

which means that H_{eff} and ρ have a common eigenbasis. Thus the optimization of $\mathcal{L}$ with respect to ρ boils down to the condition that the matrix elements of ρ coincide with those calculated for the single-particle effective Hamiltonian

$$\hat{H}_{\text{eff}} = \sum_{ij,ab,\alpha\beta} \frac{\partial L}{\partial \left[\rho_{ij}\right]^{ab}_{\alpha\beta}} \hat{a}^\dagger_{i\alpha} \hat{b}_{i\beta}, \quad (3.28)$$

which, assuming (discrete) translational invariance, can be diagonalised in the (quasi) momentum space

$$\hat{H}_{\text{eff}} = \sum_{\mathbf{k}\gamma} \tilde{\epsilon}_{\mathbf{k}\gamma} \hat{d}^{\dagger}_{\mathbf{k}\gamma} \hat{d}_{\mathbf{k}\gamma}, \tag{3.29}$$

where $\hat{d}^{\dagger}_{\mathbf{k}\gamma}$ are creation operators of quasiparticles of the effective Hamiltonian and can be expressed as a linear combination of operators $\{\hat{a}^{\dagger}_{\mathbf{k}\alpha}\}_{a,\alpha}$, where $a \in \{c, f\}$ in the normal case and $a \in \{c, f, \hat{c}^{\dagger}, \hat{f}^{\dagger}\}$ in superconducting case, since then we allow for a mixing of particle and hole states. The subscript $\mathbf{k}$ denotes Fourier-transformed operators

$$\hat{a}^{\dagger}_{\mathbf{k}\alpha} = \frac{1}{\sqrt{N}} \sum_{j} e^{i\,\mathbf{R}_j \mathbf{k}} \hat{a}^{\dagger}_{j\alpha}, \tag{3.30}$$

where $\mathbf{R}_j$ is a location of j-th lattice site. Then, the expectation values in the Fermi-sea ground state of H_{eff} are given by

$$\left\langle \hat{d}^{\dagger}_{\mathbf{k}\gamma} \hat{d}_{\mathbf{k}\gamma} \right\rangle_0 = \lim_{T \to 0} \frac{1}{e^{\tilde{\epsilon}_{\mathbf{k}\gamma}/T} + 1} \tag{3.31}$$

Formally, this is just a Heaviside theta function, however it is useful to regularize it during the numerical calculations by some small non-zero value of T. All the other expectation values are obtained by transforming the operators d from $\mathbf{k}$-space back into the operators c and f in real space. For the explicit discussion of the application of this procedure to the considered model, see Section 3.2.4.

To conclude, we enlist all the equations necessarily satisfied by the optimal variational wave-function:

1. "λ-equations": (3.22),
2. "η-equations": (3.11) and (3.12),
3. "ρ-equations": (3.19) where r.h.s comes from (3.28), (3.29) and (3.31),
4. "μ-equation": (3.21).

3.2 Application to the degenerate Anderson lattice model

Now we discuss the variational space in which we look for the optimal solutions for the two-orbital Anderson lattice model, considered in this thesis. We apply the following constraints on the variational wave-function

1. it is spatially uniform, i.e. all the quantities defined in the previous section depending on the site i are assumed to be the same,
2. it is orbitally symmetric, i.e. it is symmetric with respect to the interchange of indices $l = 1, 2$.

However, we allow for the spin-symmetry-broken states. In the following we drop the index i where it is unnecessary.

3.2.1 Gutzwiller variational parameters

In the case of the considered model, there are two correlated f-orbitals per site. The definition of the states of the local basis is presented in Table 3.1. Since we assume that the matrix of Gutzwiller parameters λ is real and symmetric, we should perform the minimization with respect to 120 different variational

parameters. In order to reduce this number and make the calculations more tractable we follow the approach of [29].

Table 3.1: Local Fock basis for two f-orbitals

I	$\|I\rangle = \|I_1, I_2\rangle$	I	$\|I\rangle = \|I_1, I_2\rangle$	I	$\|I\rangle = \|I_1, I_2\rangle$
1	$\|0, 0\rangle$	6	$\|\uparrow\downarrow, 0\rangle$	12	$\|\uparrow\downarrow, \uparrow\rangle$
2	$\|\uparrow, 0\rangle$	7	$\|0, \uparrow\downarrow\rangle$	13	$\|\uparrow\downarrow, \downarrow\rangle$
3	$\|\downarrow, 0\rangle$	8	$\|\uparrow, \uparrow\rangle$	14	$\|\uparrow, \uparrow\downarrow\rangle$
4	$\|0, \uparrow\rangle$	9	$\|\downarrow, \downarrow\rangle$	15	$\|\downarrow, \uparrow\downarrow\rangle$
5	$\|0, \downarrow\rangle$	10	$\|\uparrow, \downarrow\rangle$	16	$\|\uparrow\downarrow, \uparrow\downarrow\rangle$
		11	$\|\downarrow, \uparrow\rangle$		

First, we find the atomic eigenstates of the local interaction Hamiltonian $\hat{H}^i_{\text{int}}$ ($\hat{H}_{\text{int}} = \sum_i \hat{H}^i_{\text{int}}$), which are simultaneous eigenstates of the full f-part of the local Hamiltonian. Now, in the basis of those eigenstates we choose λ to be diagonal and each diagonal term corresponds to a given eigenstate, as shown in Table 3.2. Due to the orbital symmetry restriction, not all of those terms are independent. Now we perform the transformation of λ back to the original $\{|I\rangle\}_I$ basis, so λ acquires some non-diagonal elements.

Table 3.2: Atomic eigenstates of $\hat{H}^i_{\text{int}}$ and corresponding eigenenergies and variational parameters

Eigenstate $\|\Gamma\rangle$	$E_{\text{int},\Gamma}$	Variational parameter λ_Γ
$\|1\rangle$	0	λ_e
$\|2\rangle$	0	$\lambda_{s\uparrow}$
$\|3\rangle$	0	$\lambda_{s\downarrow}$
$\|4\rangle$	0	$\lambda_{s\uparrow}$
$\|5\rangle$	0	$\lambda_{s\downarrow}$
$\frac{1}{\sqrt{2}}(\|6\rangle + \|7\rangle)$	$U + J'$	$\lambda_{d,a}$
$\frac{1}{\sqrt{2}}(\|6\rangle - \|7\rangle)$	$U - J'$	$\lambda_{d,b}$
$\frac{1}{\sqrt{2}}(\|10\rangle - \|11\rangle)$	$U' + J$	$\lambda_{d,c}$
$\|8\rangle$	$U' - J$	$\lambda_{d\uparrow}$
$\frac{1}{\sqrt{2}}(\|10\rangle + \|11\rangle)$	$U' - J$	$\lambda_{d,0}$
$\|9\rangle$	$U' - J$	$\lambda_{d\downarrow}$
$\|12\rangle$	$U + 2U' - J$	$\lambda_{t\uparrow}$
$\|13\rangle$	$U + 2U' - J$	$\lambda_{t\downarrow}$
$\|14\rangle$	$U + 2U' - J$	$\lambda_{t\uparrow}$
$\|15\rangle$	$U + 2U' - J$	$\lambda_{t\downarrow}$
$\|16\rangle$	$2U + 4U' - 2J$	λ_f

If these were all the elements of λ, then they would have a simple interpretation. Namely, $|\lambda_\Gamma|^2$ would be a relative probability of an occupied eigenstate Γ in $|\Psi_G\rangle$ with respect to $|\Psi_0\rangle$.

Now we turn to discussing the additional entries of λ needed when we allow for local spin-triplet pairing:

$$\left\langle \hat{f}^{\dagger}_{i1\sigma}\hat{f}^{\dagger}_{i2\sigma}\right\rangle \neq 0.$$

In that case the constraints (3.12) have to be supplemented by

$$\left\langle \hat{P}_i^2\hat{f}^{\dagger}_{i1\sigma}\hat{f}^{\dagger}_{i2\sigma}\right\rangle_0 = \left\langle \hat{f}^{\dagger}_{i1\sigma}\hat{f}^{\dagger}_{i2\sigma}\right\rangle_0 \tag{3.32}$$

because the orbital basis is no longer diagonal. One should keep in mind that the number of variational parameters in λ has to exceed the number of constraint equations. Therefore, in order not to reduce our variational freedom, we are forced to introduce at least as many new variational parameters as there are new constraint equations (3.32). We introduce a variational parameter for each non-vanishing element $\langle I|\hat{f}^{\dagger}_{i1\sigma}\hat{f}^{\dagger}_{i2\sigma}|I'\rangle$ and $\langle I|\hat{f}_{i2\sigma}\hat{f}_{i1\sigma}|I'\rangle$. Again, the independent ones are chosen in a way that does not lead to the orbital symmetry breaking.

We enlist all the non-zero elements of λ in Table 3.3.

Table 3.3: Non-zero entries of the variational matrix λ. Only the elements for which $I \leq I'$ are listed.

I	I'	$\lambda_{II'}$	I	I'	$\lambda_{II'}$	I	I'	$\lambda_{II'}$
1	1	λ_e	9	9	$\lambda_{d\downarrow}$	1	8	$\lambda_{ed\uparrow}$
2	2	$\lambda_{s\uparrow}$	10	10	$\frac{1}{2}(\lambda_{d,0}+\lambda_{d,c})$	1	9	$\lambda_{ed\downarrow}$
3	3	$\lambda_{s\downarrow}$	10	11	$\frac{1}{2}(\lambda_{d,0}-\lambda_{d,c})$	2	13	$\lambda_{s\uparrow t\downarrow}$
4	4	$\lambda_{s\uparrow}$	11	11	$\frac{1}{2}(\lambda_{d,0}+\lambda_{d,c})$	3	12	$-\lambda_{s\downarrow t\uparrow}$
5	5	$\lambda_{s\downarrow}$	12	12	$\lambda_{t\uparrow}$	4	15	$-\lambda_{s\uparrow t\downarrow}$
6	6	$\frac{1}{2}(\lambda_{d,a}+\lambda_{d,b})$	13	13	$\lambda_{t\downarrow}$	5	14	$\lambda_{s\downarrow t\uparrow}$
6	7	$\frac{1}{2}(\lambda_{d,a}-\lambda_{d,b})$	14	14	$\lambda_{t\uparrow}$	8	16	$\lambda_{d\uparrow f}$
7	7	$\frac{1}{2}(\lambda_{d,a}+\lambda_{d,b})$	15	15	$\lambda_{t\downarrow}$	9	16	$\lambda_{d\downarrow f}$
8	8	$\lambda_{d\uparrow}$	16	16	λ_f			

3.2.2 Single-particle density matrix elements

Here we list all all the non-vanishing elements of the single-particle density matrix ρ which appear in the calculation of L. We explicitly set them site- and orbital-independent, while keeping the spin dependency. We also assume all of them are real numbers. Besides the diagonal elements

$$n^0_{f\sigma} \equiv \left\langle \hat{f}^{\dagger}_{il\sigma}\hat{f}_{il\sigma}\right\rangle_0, \tag{3.33}$$

$$n_{c\sigma} \equiv \left\langle \hat{c}^{\dagger}_{il\sigma}\hat{c}_{il\sigma}\right\rangle_0, \tag{3.34}$$

there are also fc hybridization amplitudes

$$v^0_{\sigma} \equiv \left\langle \hat{f}^{\dagger}_{il\sigma}\hat{c}_{il\sigma}\right\rangle_0, \tag{3.35}$$

and f and fc local spin-triplet pairing amplitudes

$$A^0_{f\sigma} \equiv \left\langle \hat{f}^\dagger_{i1\sigma} \hat{f}^\dagger_{i2\sigma} \right\rangle_0 , \tag{3.36}$$

$$A^0_{fc\sigma} \equiv \left\langle \hat{f}^\dagger_{i1\sigma} \hat{c}^\dagger_{i2\sigma} \right\rangle_0 = \left\langle \hat{c}^\dagger_{i1\sigma} \hat{f}^\dagger_{i2\sigma} \right\rangle_0 . \tag{3.37}$$

We neglect the $m_z = 0$ zero component of spin-triplet pairing amplitude since in the spin-polarized state this channel will not be preferred [15, 16].

Among the terms we need to take into account are also hopping amplitudes $\langle \hat{c}^\dagger_{il\sigma} \hat{c}_{jl\sigma} \rangle$. However, since they are only needed for the calculation of the expectation value of the hopping term $\hat{H}_c$, we do not evaluate them individually but rather transform whole $\hat{H}_c$ to $\mathbf{k}$-space, where it reads

$$\hat{H}_c = \sum_{\mathbf{k}\alpha} \epsilon_{\mathbf{k}} \, \hat{c}^\dagger_{\mathbf{k}\alpha} \hat{c}_{\mathbf{k}\alpha} \tag{3.38}$$

with the dispersion $\epsilon_{\mathbf{k}}$ given by

$$\epsilon_{\mathbf{k}} = \sum_j t_{0j} e^{i\mathbf{R}_j \mathbf{k}}. \tag{3.39}$$

Note that $n_{c\sigma}$ in (3.34) lacks "0" superscript. This is because, as explained above, expectation values of any c-only operators are the same in the both states $|\Psi_0\rangle$ and $|\Psi_G\rangle$.

3.2.3 Lagrange multipliers

In order to satisfy constraints (3.11) and (3.12) we introduce a set η of 5 Lagrange multipliers. The first of them, η_0, multiplies the term enforcing the normalization condition (3.11)

$$\eta_0 \left(\left\langle \hat{P}^2_i \right\rangle_0 - 1 \right). \tag{3.40}$$

The pair of multipliers $\eta_{1\sigma}$ enforces the diagonal part of conditions (3.12)

$$\eta_{1\sigma} \left(\left\langle \hat{P}^2_i \hat{f}^\dagger_{i1\sigma} \hat{f}_{i1\sigma} \right\rangle_0 - n^0_{f\sigma} \right). \tag{3.41}$$

Since we assume orbital equivalence, it is enough to only put a condition on the filling of $l = 1$ orbital, while the constraint for $l = 2$ is automatically fulfilled. Another pair of multipliers $\eta_{2\sigma}$ enforces the non-diagonal condition (3.32)

$$\eta_{2\sigma} \left(\left\langle \hat{P}^2_i \hat{f}^\dagger_{i1\sigma} \hat{f}^\dagger_{i2\sigma} \right\rangle_0 - A^0_{f\sigma} \right). \tag{3.42}$$

All the 5 terms defined by (3.40), (3.41) and (3.42) shall be then included in the functional L.

3.2.4 Effective single-particle Hamiltonian

Now we discuss the determination of the effective Hamiltonian $\hat{H}_{\text{eff}}$ and its diagonalization in the concrete case of our model.

We find the elements of $\hat{H}_{\text{eff}}$ from equation (3.28), by linearisation of the functional L in the single-particle density matrix ρ. The elements of ρ on which

the functional L depends are listed in Section 3.2.2. Then, using (3.30) all the local elements of ρ are transformed into constant terms in $\mathbf{k}$-space and the only non-local contribution coming from $\hat{H}_c$ is that given by (3.38) and (3.39). Consequently, we obtain the following $\hat{H}_{\text{eff}}$ in $\mathbf{k}$-space, which we present in a convenient Nambu notation

$$\hat{H}_{\text{eff}} = \sum_{\mathbf{k}\sigma} \begin{pmatrix} \hat{c}^\dagger_{\mathbf{k}1\sigma} \\ \hat{c}_{-\mathbf{k}2\sigma} \\ \hat{f}^\dagger_{\mathbf{k}1\sigma} \\ \hat{f}_{-\mathbf{k}2\sigma} \end{pmatrix}^{\mathrm{T}} \begin{pmatrix} \epsilon_{\mathbf{k}} - \mu & 0 & \tilde{V}_\sigma & \tilde{\Delta}_{fc\sigma} \\ 0 & -\epsilon_{\mathbf{k}} + \mu & \tilde{\Delta}_{fc\sigma} & -\tilde{V}_\sigma \\ \tilde{V}_\sigma & \tilde{\Delta}_{fc\sigma} & \tilde{\epsilon}_{f\sigma} & \tilde{\Delta}_{f\sigma} \\ \tilde{\Delta}_{fc\sigma} & -\tilde{V}_\sigma & \tilde{\Delta}_{f\sigma} & -\tilde{\epsilon}_{f\sigma} \end{pmatrix} \begin{pmatrix} \hat{c}_{\mathbf{k}1\sigma} \\ \hat{c}^\dagger_{-\mathbf{k}2\sigma} \\ \hat{f}_{\mathbf{k}1\sigma} \\ \hat{f}^\dagger_{-\mathbf{k}2\sigma} \end{pmatrix}. \tag{3.43}$$

The effective energies are defined by

$$\tilde{\epsilon}_{f\sigma} \equiv \frac{1}{2}\frac{\partial L}{\partial n^0_{f\sigma}}, \tag{3.44}$$

$$\tilde{V}_\sigma \equiv \frac{1}{4}\frac{\partial L}{\partial v^0_\sigma}, \tag{3.45}$$

$$\tilde{\Delta}_{f\sigma} \equiv \frac{1}{2}\frac{\partial L}{\partial A^0_{f\sigma}}, \tag{3.46}$$

$$\tilde{\Delta}_{fc\sigma} \equiv \frac{1}{4}\frac{\partial L}{\partial A^0_{fc\sigma}}, \tag{3.47}$$

where the numerical factors ensure we are not over-counting single-particle contributions due to degeneracy of particular density matrix elements. Note that the chemical potential μ for f-level is already incorporated in the functional L.

In the case of Hartree-Fock approximation, to which the Gutzwiller approximation reduce in the limit $\lambda = \mathbb{1}, \eta = \mathbb{0}$, those elements of the effective Hamiltonian read

$$\tilde{\epsilon}_{f\sigma} = \epsilon_f + (U + U')n^0_{f\bar{\sigma}} + \left(U' - J\right) n^0_{f\sigma} - \mu, \tag{3.48}$$

$$\tilde{V}_\sigma = V, \tag{3.49}$$

$$\tilde{\Delta}_{f\sigma} = (U' - J)A^0_{f\sigma}, \tag{3.50}$$

$$\tilde{\Delta}_{fc\sigma} = 0, \tag{3.51}$$

where $\bar{\sigma}$ denotes a spin opposite to σ. The Gutzwiller approximation leads to the renormalization of those effective Hartree-Fock parameters, in particular to the σ dependence of $\tilde{V}_\sigma$ and non-zero value of $\tilde{\Delta}_{fc\sigma}$ (see Appendix B for an explicit example).

In order to find the proper quasiparticle operators $\hat{d}^\dagger_{\mathbf{k}\gamma}$ and the corresponding energies $\tilde{\epsilon}_{\mathbf{k}\gamma}$, as in equation (3.29), the 4×4 Hamiltonian matrix from (3.43) has to be diagonalized for each $\mathbf{k}$ and σ

$$\begin{pmatrix} \epsilon_{\mathbf{k}} - \mu & 0 & \tilde{V}_\sigma & \tilde{\Delta}_{fc\sigma} \\ 0 & -\epsilon_{\mathbf{k}} + \mu & \tilde{\Delta}_{fc\sigma} & -\tilde{V}_\sigma \\ \tilde{V}_\sigma & \tilde{\Delta}_{fc\sigma} & \tilde{\epsilon}_{f\sigma} & \tilde{\Delta}_{f\sigma} \\ \tilde{\Delta}_{fc\sigma} & -\tilde{V}_\sigma & \tilde{\Delta}_{f\sigma} & -\tilde{\epsilon}_{f\sigma} \end{pmatrix} = \mathcal{U}^{\mathrm{T}}_{\mathbf{k}\sigma} \begin{pmatrix} \tilde{\epsilon}_{\mathbf{k}\sigma 1} & 0 & 0 & 0 \\ 0 & \tilde{\epsilon}_{\mathbf{k}\sigma 2} & 0 & 0 \\ 0 & 0 & \tilde{\epsilon}_{\mathbf{k}\sigma 3} & 0 \\ 0 & 0 & 0 & \tilde{\epsilon}_{\mathbf{k}\sigma 4} \end{pmatrix} \mathcal{U}_{\mathbf{k}\sigma}, \tag{3.52}$$

where $\mathcal{U}_{\mathbf{k}\sigma}$ is a unitary matrix transforming the Nambu vector of operators to the eigenbasis of $\hat{H}_{\text{eff}}$. Then the local density matrix is evaluated by the summation

over the full **k**-space

$$\begin{pmatrix} n_{c\sigma} & 0 & v^0_\sigma & A^0_{fc\sigma} \\ 0 & 1-n_{c\sigma} & A^0_{fc\sigma} & -v^0_\sigma \\ v^0_\sigma & A^0_{fc\sigma} & n^0_{f\sigma} & A^0_{f\sigma} \\ A^0_{fc\sigma} & -v^0_\sigma & A^0_{f\sigma} & 1-n^0_{f\sigma} \end{pmatrix} = \frac{1}{N}\sum_{\mathbf{k}} \mathcal{U}^{\mathrm{T}}_{\mathbf{k}\sigma} \begin{pmatrix} \tilde{n}_{\mathbf{k}\sigma 1} & 0 & 0 & 0 \\ 0 & \tilde{n}_{\mathbf{k}\sigma 2} & 0 & 0 \\ 0 & 0 & \tilde{n}_{\mathbf{k}\sigma 3} & 0 \\ 0 & 0 & 0 & \tilde{n}_{\mathbf{k}\sigma 4} \end{pmatrix} \mathcal{U}_{\mathbf{k}\sigma}, \quad (3.53)$$

where we calculate $\tilde{n}_{\mathbf{k}\gamma}$ according to (3.31)

$$\tilde{n}_{\mathbf{k}\gamma} \equiv \left\langle \hat{d}^\dagger_{\mathbf{k}\gamma} \hat{d}_{\mathbf{k}\gamma} \right\rangle_0 = \lim_{T\to 0} \frac{1}{e^{\tilde{\epsilon}_{\mathbf{k}\gamma}/T}+1}. \quad (3.54)$$

We calculate the only non-local contribution to the ground state energy $\langle \hat{H}_c \rangle$ by the summation

$$\left\langle \hat{H}_c \right\rangle = \sum_{\mathbf{k}l\sigma} \epsilon_{\mathbf{k}} \left\langle \hat{c}^\dagger_{\mathbf{k}l\sigma} \hat{c}_{\mathbf{k}l\sigma} \right\rangle = 2 \sum_{\mathbf{k}l\sigma} \left(\epsilon_{\mathbf{k}} \sum_{r=1}^{4} \left[\mathcal{U}^{\mathrm{T}}_{\mathbf{k}\sigma} \right]_{1r} \tilde{n}_{\mathbf{k}r} \left[\mathcal{U}_{\mathbf{k}\sigma} \right]_{r1} \right), \quad (3.55)$$

where factor 2 reflects the orbital degeneracy. Actually, as described in Appendix A, instead of the summation in **k**-space, we perform the integration over the density of c-states.

It should be noted that although the Hamiltonian $\hat{H}_{\mathrm{eff}}$ serves for the determination of $|\Psi_0\rangle$ or, in other words, for the calculation of the elements of the single-particle density matrix ρ, the expectation values $\langle \hat{H}_{\mathrm{eff}} \rangle$ and $\langle \hat{H} \rangle$ do not coincide.

Chapter 4

Results and discussion

In this final chapter we present and discuss our results. After a brief justification of the chosen basic set of model parameters, we carry on a discussion of the general features of the found ferromagnetic and superconducting ground states, and, in particular, provide representative solutions. Then, we compare the results of multi-band Gutzwiller approximation scheme to those obtained by Hartree-Fock method and show the deficiencies of the latter in description of the electronic correlations in the considered model. Next, we demonstrate how the solutions evolve when the model parameters are modified. In particular, we investigate how the pairing amplitude is influenced by the reduction of Hund's coupling J. At the end, we emphasise the role of electronic correlations in sustaining spin-triplet superconductivity, as well as summarize our findings.

4.1 Model parameters

To maintain a connection with previous works on the Anderson lattice model [20–22] we choose square lattice density of conduction (c) electron states with nearest neighbour ($t = 0.125\,W$) and next-nearest ($t' = 0.25\,|t|$) neighbour hopping (Fig. 4.1) resulting from the dispersion

$$\epsilon_{\mathbf{k}} = -2t(\cos k_x + \cos k_y) + 4t' \cos k_x \cos k_y. \tag{4.1}$$

However, in the forthcoming section we also show one plot obtained for the constant density of states. According to Section 2.1 we choose the bandwidth of conduction c electrons $W = 1$ as a unit of energy.

Our model study is not oriented toward any particular compound, nevertheless we try to keep values of the considered model parameters in physically reasonable ranges. In general, we present the results as functions of hybridization V. The reasons for this are that by modifying its strength we encompass all the known ferromagnetic phases of Anderson lattice model away from half filling (discussed later) and it is likely that the evolution of this parameter can emulate pressure change, often used in the studies of heavy-fermion compounds. For the first reason we sometimes present results for unreasonably high hybridization ($|V| > 1$), in order to show the boundaries of all the analysed phases.

The basic set of parameters we choose is

- $\epsilon_f = -0.5$,
- $U = 1.0$,
- $J/U = 0.5$,
- $n = 3.25$,

while keeping the relation $U' = U - 2J$. We found that f-level has to lie relatively low with respect to the centre of the conduction band if we want to observe significant pairing amplitudes, which explains the chosen value of $\epsilon_f = -0.5$.

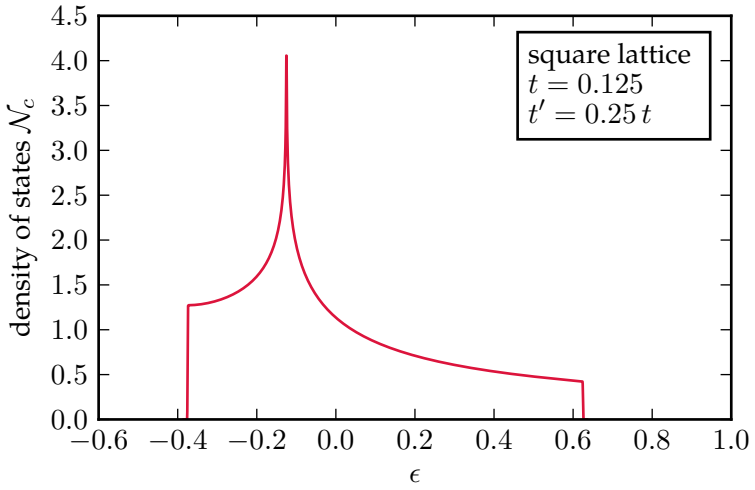

Figure 4.1: Square lattice density of states resulting from nearest ($t = 0.125$) and next-nearest ($t' = 0.25\,t$) neighbour hopping integrals. Note Van Hove singularity in the lower half of the band.

Next, because we wish to analyse the role of electronic correlations in the formation of superconducting gap, we choose a moderately large Hubbard $U = 1$. We presume that at this value of U, any approximation not taking explicitly the correlations into account, such as Hartree-Fock method, will provide at best only the qualitative features of solutions. It is reasonable to scale all the interaction terms together with U, so instead of J we keep constant the ratio $J/U = 0.5$. At first glance it seems that we set Hund's coupling J non-physically high (it implies $U' = 0$), but it lets us find the regions in the space of model parameter space which are mostly prone to spin-triplet superconductivity. Finally, since Anderson lattice model is believed to exhibit ferromagnetism only away from half filling, we choose $n = 3.25$, which also ensures that in the ground state there will be sufficiently large contribution from double f-occupancies, necessary for the local pairing. It is worth mentioning that the results of our approach may be compared to those of [20] upon the proper scaling of the obtained here magnetizations and fillings to the orbitally non-degenerate case. Therefore the chosen microscopic parameters lie in the close vicinity to ones in that work.

4.2 Results

4.2.1 General features of ground states

In Fig. 4.2 we plot the following quantities for the base parameters of the model as f of functions of hybridization V:

- average occupancies (fillings) of f- and c-electrons per orbital

$$n_f \equiv \sum_\sigma \langle \hat{n}^f_{il\sigma} \rangle, \tag{4.2}$$

$$n_c \equiv \sum_\sigma \langle \hat{n}^c_{il\sigma} \rangle, \tag{4.3}$$

- magnetization of f and c electrons, and the total magnetization m

$$m_f \equiv \frac{1}{2}\sum_l \Big(\langle \hat{n}^f_{il\uparrow}\rangle - \langle \hat{n}^f_{il\downarrow}\rangle\Big), \tag{4.4}$$

$$m_c \equiv \frac{1}{2}\sum_l \Big(\langle \hat{n}^c_{il\uparrow}\rangle - \langle \hat{n}^c_{il\downarrow}\rangle\Big), \tag{4.5}$$

$$m \equiv m_f + m_c, \tag{4.6}$$

- local spin-triplet inter-orbital pairing amplitudes $A_{f\uparrow}$, $A_{f\downarrow}$

$$A_{f\sigma} \equiv \langle \hat{f}^\dagger_{i1\sigma}\hat{f}^\dagger_{i2\sigma}\rangle, \tag{4.7}$$

- ground state energy E_{G} per lattice site

$$E_{\mathrm{G}} \equiv \frac{\langle \hat{H}\rangle}{N}, \tag{4.8}$$

- condensation energy ΔE, i.e. the difference of ground state energies between ferromagnetic (paramagnetic) normal and ferromagnetic (paramagnetic) superconducting phase, defined e.g as

$$\Delta E \equiv E_{\mathrm{G}}(\mathrm{FM}) - E_{\mathrm{G}}(\mathrm{FMSC}), \tag{4.9}$$

- renormalization factors $Q_\uparrow$, $Q_\downarrow$, which are indicators of the correlations strength (the lower their values, the stronger the correlations)

$$Q_\sigma \equiv \left(\frac{\tilde{V}_\sigma}{V}\right)^2. \tag{4.10}$$

Before moving on to the discussion of pairing amplitudes, we discuss the magnetic phases present in the considered V parameter range (Fig. 4.2a). Our analysis is supplemented by Fig. 4.3 in which we plot the effective Landau-Gutzwiller quasiparticle spin-resolved density of states $\mathcal{N}_\sigma(\epsilon)$, being defined by

$$\mathcal{N}_\sigma(\epsilon) \equiv \frac{2}{N}\sum_{\mathbf{k},r=1,3} \delta(\epsilon - \tilde{\epsilon}_{\mathbf{k}\sigma r}), \tag{4.11}$$

where $\tilde{\epsilon}_{\mathbf{k}\sigma r}$ are the effective single-particle energies defined in (3.52), $r = 1, 2, 3, 4$ enumerates the effective particle- and hole-like quasiparticle states and the summation is restricted only to the particle-like ones. Then the expression has to be multiplied by 2 in order to ensure the proper normalization. One can actually show that this is an appropriate density of quasiparticle states within the correlated Gutzwiller wave-function [50].

At low values of hybridizations we observe a strongly magnetically saturated phase, which we call FM2. In this phase, f-electrons hybridize with c-electrons only weakly and Hubbard interaction U as well as U' and J introduce a substantial energy splitting between spin-up and spin-down f-like effective hybridized quasiparticles. This results in a completely filled low-lying spin-up f-level. When the hybridization is increased, the low-lying f-level acquires more c-electron admixture and gradually turns into the lower spin-up hybridized subband, which is separated by a gap from the upper subband being composed mainly of conduction electrons (Fig. 4.3a). In this regime, the filling of f-orbitals n_f differs

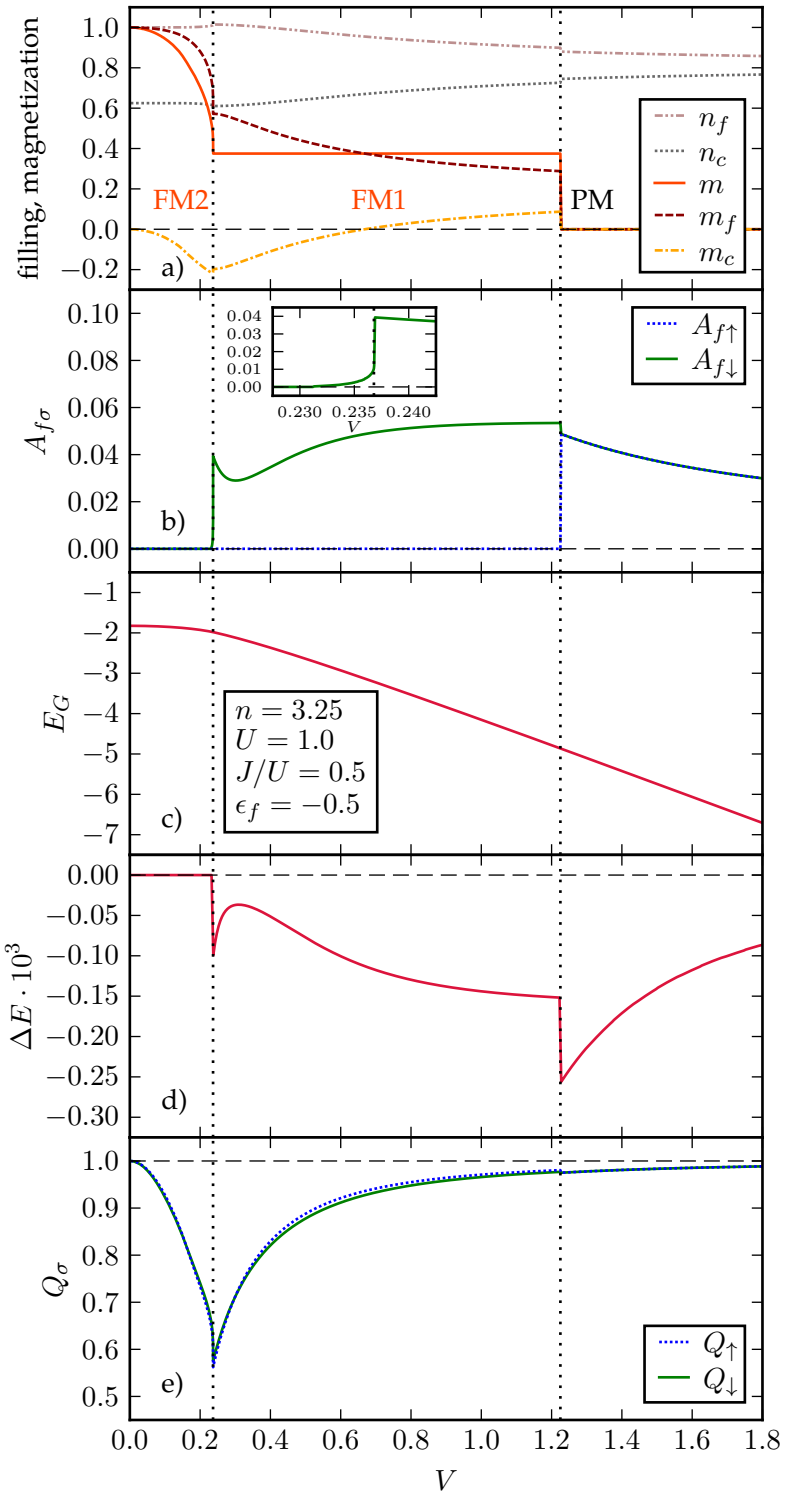

Figure 4.2: a) Fillings and magnetizations of c- and f- states, and the total magnetization m, b) pairing amplitudes $A_{f\sigma}$, c) ground state energy E_{G}, d) superconducting condensation energy ΔE, e) renormalization factors Q_σ, all as functions of hybridization V for $n = 3.25, U = 1.0, J/U = 0.5, \epsilon_f = -0.5$ and the square lattice density of c-states

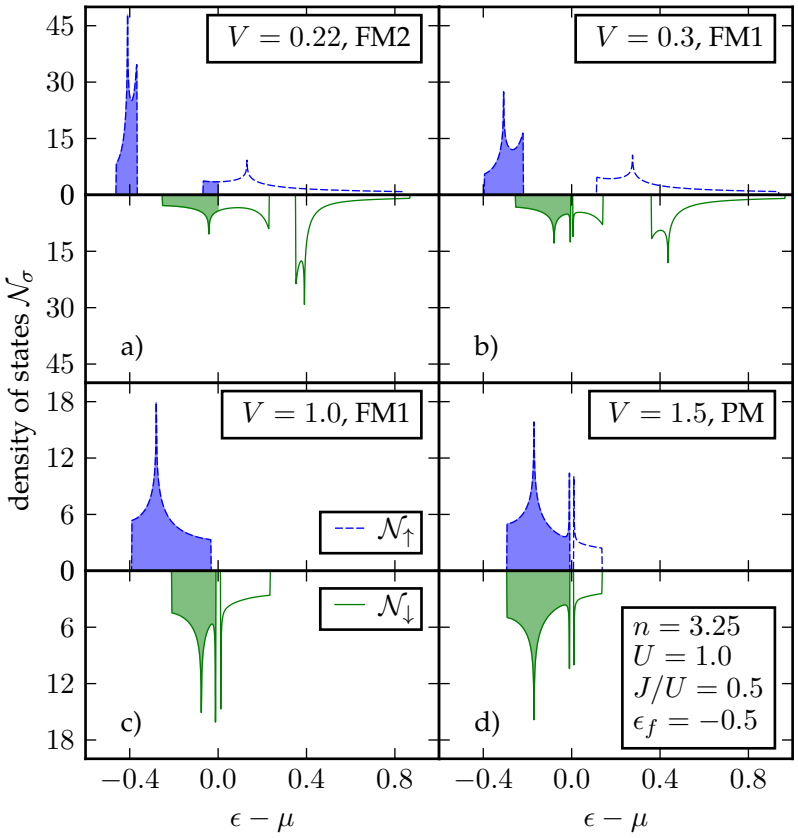

Figure 4.3: Spin-resolved density of Landau-Gutzwiller quasiparticle states $\mathcal{N}_\sigma$ for hybridizations a) $V = 0.22$ (FM2), b) $V = 0.3$ (FM1), c) $V = 1.0$ (FM1), d) $V = 1.5$ (PM phase), all for $n = 3.25$, $U = 1.0$, $J/U = 0.5$, $\epsilon_f = -0.5$ and the square lattice density of c-states. Shaded areas denote occupied states lying below the Fermi energy (chemical potential μ).

only slightly from unity, indicating an almost localized nature of f-electrons. The local f-moments are partially screened by the negative spin polarization of itinerant c-electrons.

Further increase of the hybridization leads to the widening of the gap between the both subbands. At a certain value of V the hybridization gap is such large that the upper spin-up subband becomes empty. This marks the beginning of the weakly saturated *half-metallic ferromagnetic* phase, which we call briefly FM1. In this phase the lower spin-up subband is completely filled and the remaining electron filling originates only from the lower spin-down subband (Fig. 4.3b). It is interesting that one can derive a relation between the total electron filling n and magnetization m in FM1 phase. Namely, because the total electron number per site is (on average) conserved ($n = n_\uparrow + n_\downarrow$) and the number of spin-up electrons is fixed to two (each subband contains up to two electrons due to orbital degeneracy), we have

$$m = \frac{1}{2}(n_\uparrow - n_\downarrow) = 2 - \frac{n}{2}. \tag{4.12}$$

When the hybridization is increased even further, the splitting between spin-up and spin-down subbands is decreased, because the f-like hybridized quasi-particles become more and more delocalized and correlation effects are being gradually diminished (Fig. 4.3c). Finally, we observe an abrupt transition to paramagnetic phase (PM), where spin-up and spin-down states become degenerate (Fig. 4.3d).

Now, we turn our discussion to the local spin-triplet inter-orbital f-electron pairing amplitudes $A_{f\sigma}$. While in phase FM2 we hardly observe any superconductivity, there is quite a robust spin-down pairing amplitude in the half-metallic FM1 phase. As shown in the inset in Fig. 4.2b, this amplitude also extends to FM2 phase, however it decreases very quickly away from the transition point. In the paramagnetic phase we observe the same strength of pairing in both spin channels, which decreases with the increasing V.

The reason for no spin-up pairing in FM1 phase is its half-metallicity - there is no spin-up density of states at the chemical potential μ, hence no superconducting gap in the spin-up spectrum can be formed. What is important, in this phase we distinguish two types of superconducting regimes, which are separated by the pairing amplitude minimum around $V = 0.3$: the first one around FM2-FM1 border, at which pairing amplitude is visibly enhanced and the second one, extending from FM1-PM transition point in the direction of lower V, in which pairing amplitude is slowly varying. The result obtained for the basic set of parameters, which we have introduced in the previous section, is actually unique, since we observe both types of superconductivity in FM1 phase. As we will see, changing some of the model parameters may lead to the observation of only one of those two types of superconducting regimes in V-dependent plots.

The spin-triplet superconducting gaps are very narrow and hardly visible in the plots in Fig. 4.3. This is reflected in the values of the condensation energy ΔE, whose magnitude is only of the order of $10^{-4}\,W$. Thus the predicted superconducting gap formation will be possible only at very low temperatures.

What may be troubling to some extent, are the apparent energy jumps at both magnetic phase transitions present in Fig. 4.2d. However, we believe they are just very steep crossovers. We presume it from the inset showing that $A_{f\downarrow}$ decreases very quickly to zero in FM2 but nevertheless in a continuous manner. To clarify the nature of FM1-PM transition, in Fig. 4.4 we present a corresponding result obtained for the constant density of conduction states and slightly modified model parameters. In this case we observe an additional crossover phase, named FM0, between FM1 and PM. Ferromagnetically ordered phase FM0, in contrast to FM1, is characterized by the non-vanishing density of states at Fermi level for both spin populations and continuously connects FM1 with PM. Such a phase has also been reported in a recent study of non-degenerate Anderson lattice model using a Gutzwiller-like method [51]. It is interesting to note that in this phase both pairing amplitudes are non-zero and they differ from each other. The hypothesis we put forward is that this phase is also present in the case of the square lattice density of conduction states, although it is too narrow to be found. In this respect, we are not able to make a strong statement about the nature of FM1-PM transition.

Finally, we draw the reader's attention to the renormalization factors Q_σ (Fig. 4.2e). While in the limits $V = 0$ and $V \to \infty$ they approach unity (no renormalization), they differ from unity in the neighbourhood of FM2-FM1 phase transition. Hence, this is a region of the strongest electronic correlations.

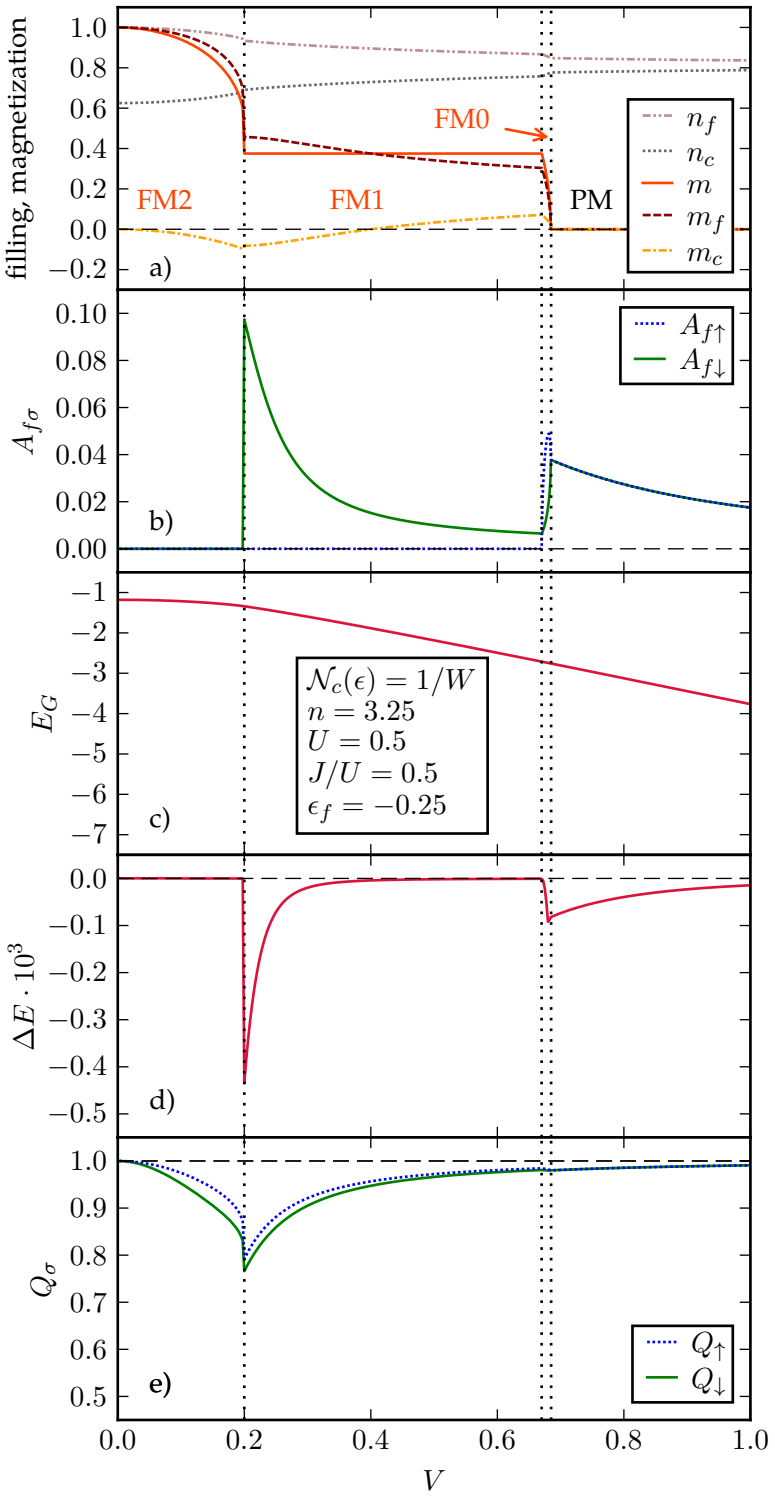

Figure 4.4: a) Fillings and magnetizations of c- and f- states, and the total magnetization m, b) pairing amplitudes $A_{f\sigma}$, c) ground state energy E_{G}, d) superconducting condensation energy ΔE, e) renormalization factors Q_σ, all as functions of hybridization V for $n = 3.25$, $U = 0.5$, $J/U = 0.5$, $\epsilon_f = -0.25$ and constant density of c-states $\mathcal{N}_c(\epsilon) = 1/W$ in the interval $[-W/2, W/2]$

4.2.2 Comparison to Hartree-Fock method

Here we compare our result from Fig. 4.2, based on the multi-band Gutzwiller approximation, to the corresponding result obtained within the Hartree-Fock method (Fig. 4.5), which is equivalent to setting $\lambda = \mathbb{1}$ (identity matrix), $\eta = \mathbb{0}$ within the current formalism.

The sequence of phases is exactly the same, although the following differences are noteworthy. First, the FM2-FM1 phase transition is much sharper in the case of Gutzwiller approximation due to strong electronic correlations in its neighbourhood. Also, the Hartree-Fock solution for $U = 1.0$ does not exhibit superconductivity in this region, while the Gutzwiller wave-function solution does. We think that the superconducting instability in the neighbourhood of this phase transition is actually sustained by electronic correlations, since the renormalization factors Q_σ differ significantly from 1 precisely in this regime.

The Hartree-Fock result for $U = 0.5$ is interesting because of a significant extension of superconductivity into FM2 phase. Actually, the $U = 0.5$ solutions within Hartree-Fock and Gutzwiller approximations are not very different. This can be seen from the relative energy gain $E_{\mathrm{HF}} - E_{\mathrm{G}}$ in the Gutzwiller wave-function solution (Fig. 4.5d), which is (on average) much larger in the case $U = 1.0$. Again, the energy gain in both cases is largest around the aforementioned FM2-FM1 phase transition, where correlation effects are most important.

4.2.3 Model parameter dependence

Here we present how the base solutions for the total magnetization m and the spin-down pairing amplitude $A_{f\downarrow}$ change when the parameters n, ϵ_f and U are varied.

First, we investigate the ϵ_f dependence (Fig. 4.6). As already mentioned, the lowering of ϵ_f leads to stronger pairing amplitudes. Although, the value of pairing amplitude is high around FM2-FM1 border for $\epsilon_f = -0.75$, the maximum of $A_{f\downarrow}$ around $V = 0.4$ suggests that in this case we observe the second type of superconducting regime, characterized by slowly-varying and extended in V pairing amplitude, in accordance with the previously introduced classification. Although the superconductivity is much weaker in the case $\epsilon_f = -0.25$, the qualitative behaviour is similar to the base $\epsilon_f = -0.5$ case. It is interesting that the location of FM2-FM1 transition point is almost unaffected by the change of ϵ_f, while the point of transition to the paramagnetic phase moves to higher values of V with the deepening of f-level.

The modification of the total electron filling n allows for the best investigation of the two types of superconducting regimes. As is it is clearly seen in Fig. 4.7, while for $n = 3.0$ we observe an extended superconducting region starting from FM1-PM transition point (second type of superconducting regime), for $n = 3.5$ the superconductivity is noticeably enhanced at the FM2-FM1 border (first type). Again, the location of FM2-FM1 transition point does not depend on n. The value of constant magnetization m in FM1 phase agrees with equation (4.12). Lower values of n lead to FM1-PM transition at higher hybridization V.

The alteration of Hubbard interaction strength U translates into significant changes of the locations both the magnetic phase transitions (Fig. 4.8). It also enables one to observe the superconducting of the first type for $U = 0.5$ and of the second type for $U = 1.5$. The solution for $U = 0.5$ actually resembles the Hartree-Fock solution (Fig. 4.5) and similarly exhibits very high values of pairing

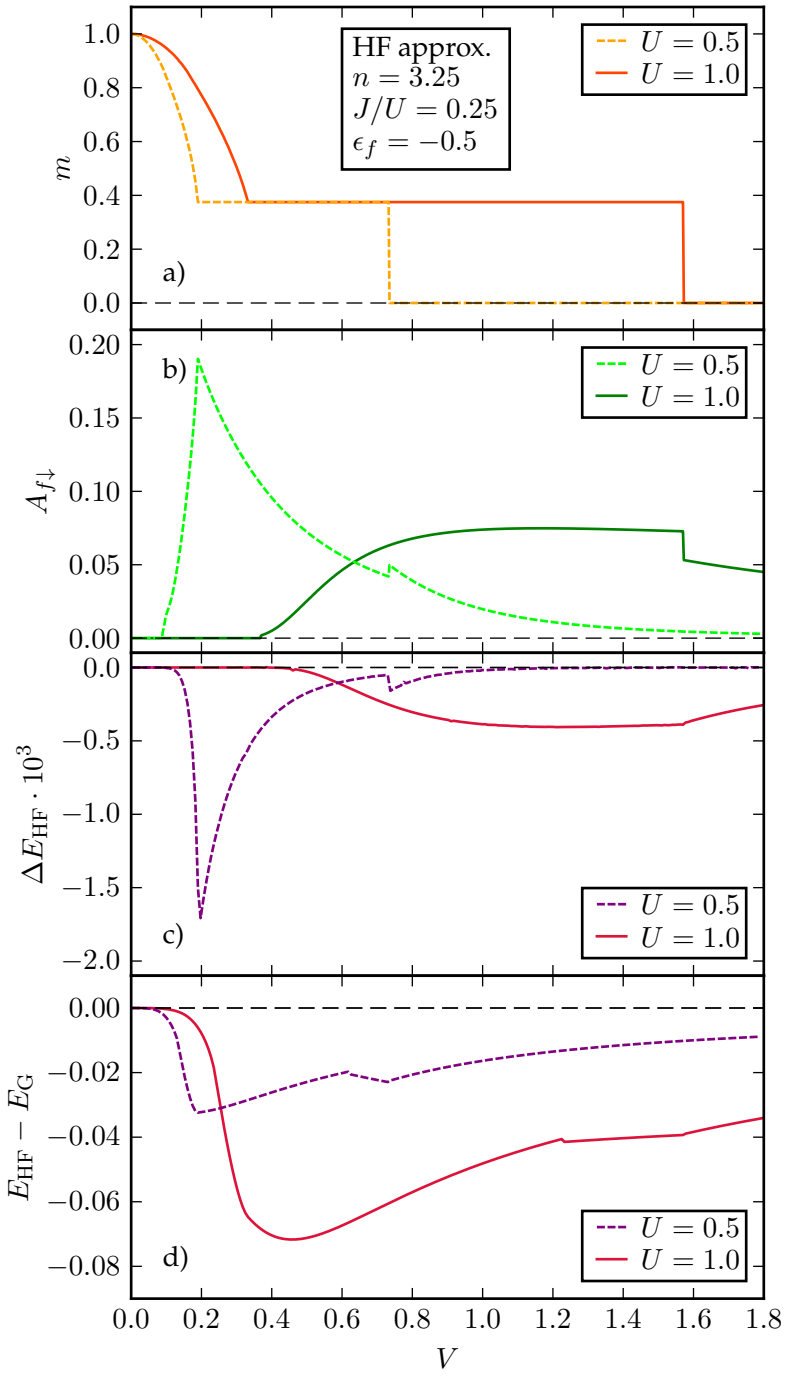

Figure 4.5: a) Total magnetization m, b) pairing amplitude $A_{f\downarrow}$, c) superconducting condensation energy ΔE_{HF}, d) difference of ground state energy with respect to Gutzwiller wave-function solution $E_{\mathrm{HF}} - E_{\mathrm{G}}$, all as functions of hybridization V for $n = 3.25$, $J/U = 0.5$, $\epsilon_f = -0.5$, $U = 0.5, 1.0$ and the square lattice density of c-states, for Hartree-Fock solution

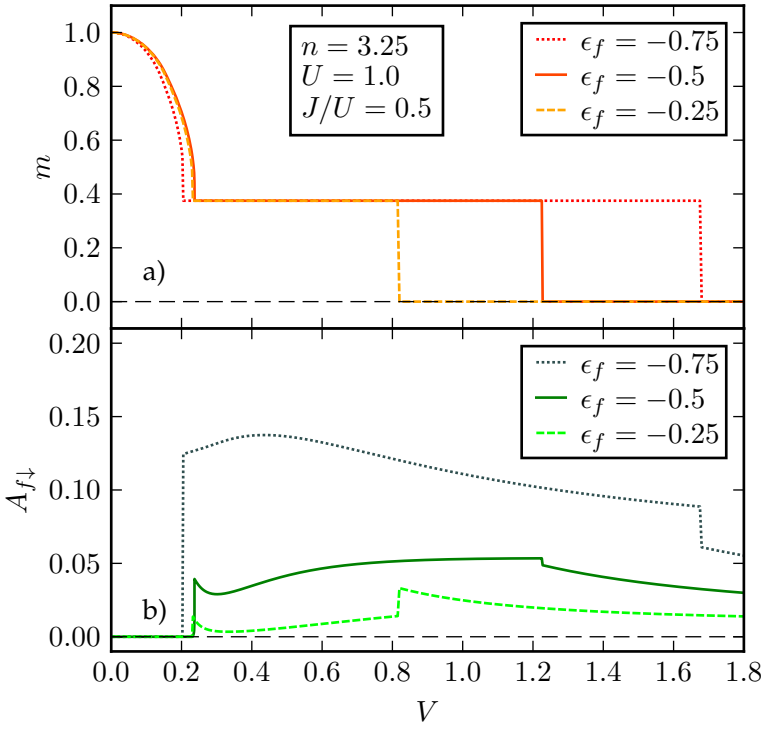

Figure 4.6: a) Total magnetization m, b) pairing amplitude $A_{f\downarrow}$ as functions of V for $n = 3.25$, $J/U = 0.5$, $U = 1.0$ and the square lattice density of c-states, for f-level energies ϵ_f = -0.75, -0.5, -0.25

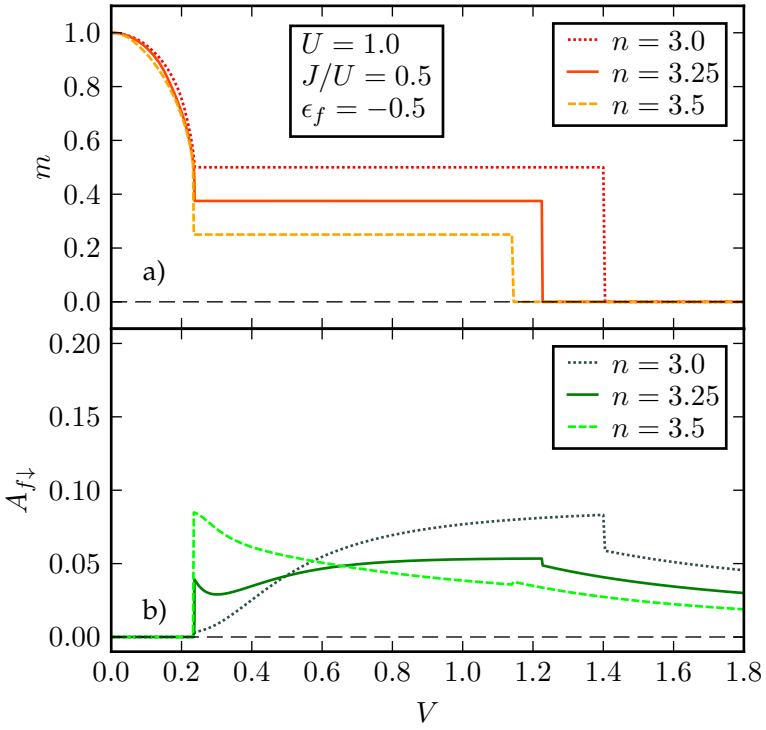

Figure 4.7: a) Total magnetization m, b) pairing amplitude $A_{f\downarrow}$ as functions of V for $J/U = 0.5$, $U = 1.0$, $\epsilon_f = -0.5$ and the square lattice density of c-states, for fillings n = 3.0, 3.25, 3.5

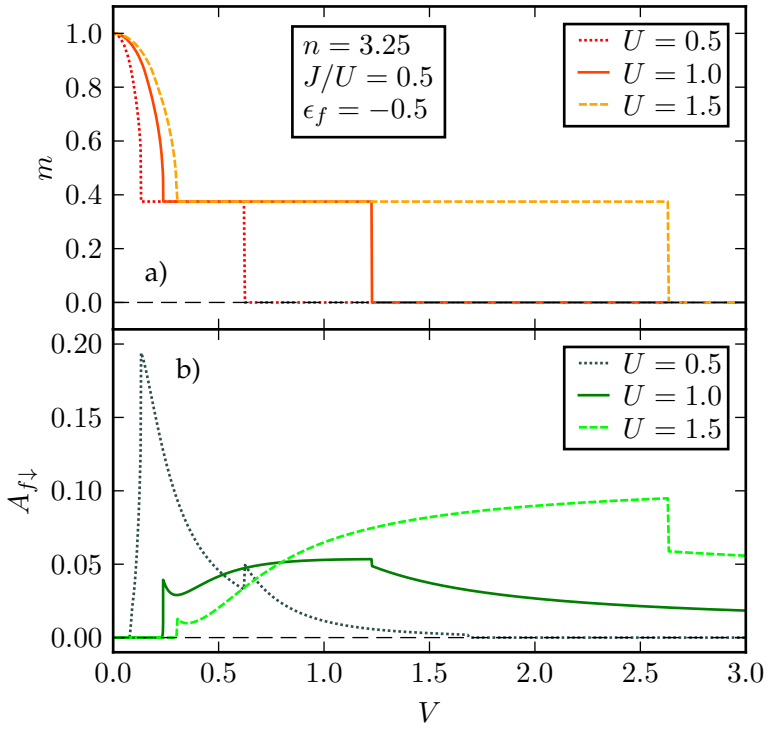

Figure 4.8: a) Total magnetization m, b) pairing amplitude $A_{f\downarrow}$ as functions of V for $n = 3.25$, $J/U = 0.5$, $\epsilon_f = -0.5$ and the square lattice density of c-states, for Hubbard interaction couplings $U = 0.5, 1.0, 1.5$

amplitude $A_{f\downarrow}$ close to FM2-FM1 border. Thus, it seems that in the regime of low U the superconductivity can exist without effects of electronic correlations.

4.2.4 Superconductivity in lower J regime

Now we would like to investigate the range of J for which the Hund's rule induced pairing is possible. Since the ratio $J/U = 0.5$ considered up to now is probably too high to be realized in an actual material, we will try to find out how much we can lower it without the destruction of the superconducting gap. The naive BCS-like consideration lead to the conclusion that pairing will occur only if the effective attractive interaction coupling between same spin f-electrons $U' - J$ will be negative, cf. equation (2.21). However, the correlation effects may allow for the pairing even when $U' > J$, or, using the relation (2.17), if $J < U/3$. Such an effect has been indeed observed in a study of spin-triplet inter-orbital pairing in two-band Hubbard model [18, 19]

We have found particularly strong spin-triplet superconductivity around FM2-FM1 transition point for $U = 1.0$ and $(n, \epsilon_f) = (3.25, -0.75), (3.5, -0.5)$. The pairing amplitude was also large for $U = 0.5$, however here we would like to focus on the influence of strong electronic correlations on the pairing amplitude. Hence, in this section we restrict ourselves to the higher value of $U = 1.0$. Now, starting from those solutions we would like to analyse the J dependence of the pairing amplitude $A_{f\uparrow}$. For the sake of this task, we choose two values of hybridization for which the pairing amplitude is relatively high: $V = 0.25$, for which correlations measured by Q_σ factors are stronger, and $V = 0.5$, for

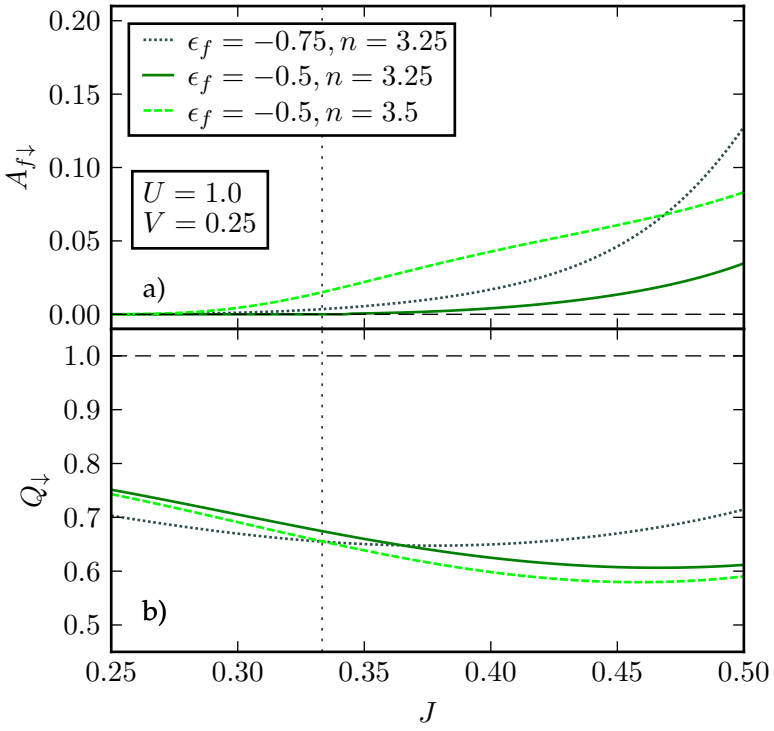

Figure 4.9: Hund's coupling J dependence of a) pairing amplitude $A_{f\downarrow}$ and b) renormalization factor $Q_\downarrow$ for $V = 0.25$, $U = 1.0$ and the square lattice density of states, for ϵ_f, n indicated in the figure. The vertical line denotes the point $J = U'$.

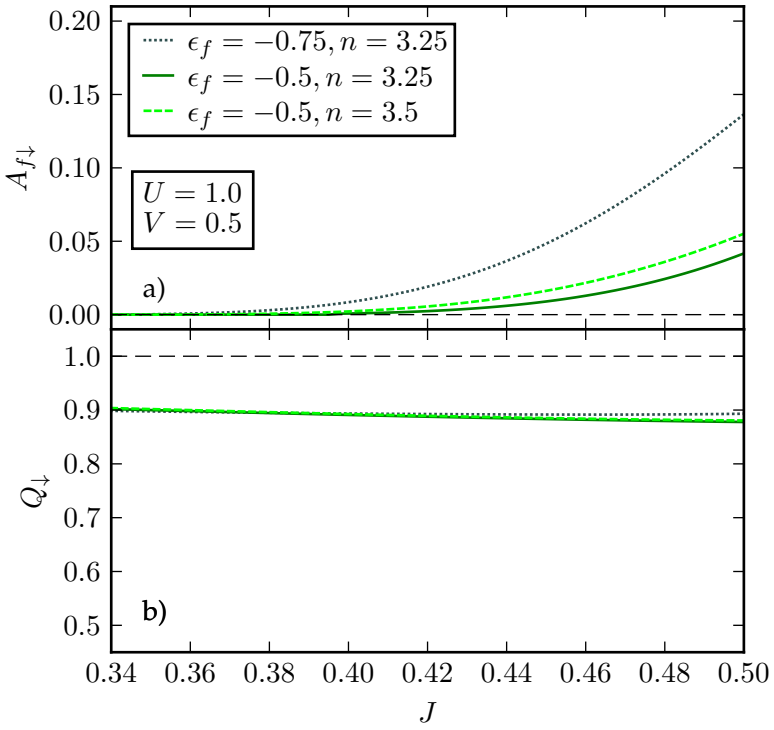

Figure 4.10: Hund's coupling J dependence of a) pairing amplitude $A_{f\downarrow}$ and b) renormalization factor $Q_\downarrow$ for $V = 0.5$, $U = 1.0$ and the square lattice density of states, for ϵ_f, n indicated in the figure

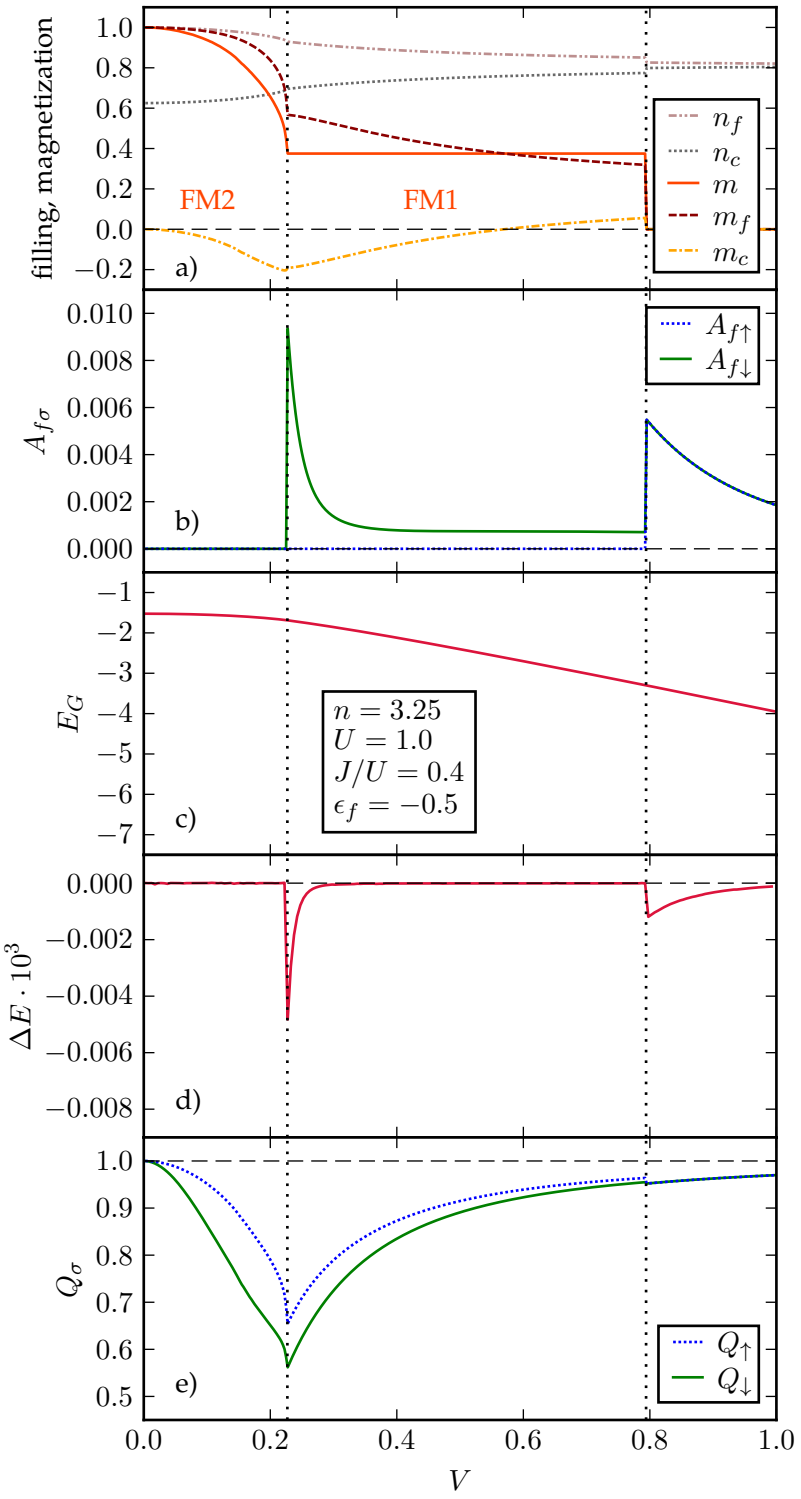

Figure 4.11: a) Fillings and magnetizations of c- and f- states, and the total magnetization m, b) pairing amplitudes $A_{f\sigma}$, c) ground state energy E_{G}, d) superconducting condensation energy ΔE, e) renormalization factors Q_σ, all as functions of hybridization V for $n = 3.25$, $U = 1.0$, $J/U = 0.4$, $\epsilon_f = -0.5$ and the square lattice density of c-states

which correlations are weaker. For those values, we plot $A_{f\downarrow}$ together with $Q_\downarrow$ as a function of J, in order to observe the role of electronic correlations in sustaining the superconducting phase.

As we expect, in the regime of strong correlations around FM2-FM1 border, the superconducting solution can persist even to the region of $J < U/3$ (Fig. 4.9), while in the domain of weaker correlations the pairing amplitude diminishes to 0 much quicker (Fig. 4.9). This is especially clearly seen for the case $(\epsilon_f, n) = (-0.5, 3.5)$, in which the pairing amplitude $A_{f\downarrow}$ at the starting point $J = 0.5$ for $V = 0.5$ is even stronger than for $V = 0.25$, nevertheless only in for the latter V it extends behind $J = U/3$. We ascribe this effect to the electronic correlations incorporated into the Gutzwiller wave-function, which are indicated by much lower value of $Q_\downarrow$ (and $Q_\uparrow$) for $V = 0.25$.

Finally, in Fig. 4.11 we present the full result for ratio $J/U = 0.4$, which can actually be considered to be more realistic. The values of the superconducting gap and condensation energy are strongly decreased with respect to $J/U = 0.5$ solution. However, the prominence of the pairing amplitude around FM2-FM1, is even more visible, which, as we postulate, is due to strong electronic correlations.

4.3 Summary and outlook

In this thesis, motivated by a need of developing a theory for the experimentally discovered heavy-fermion ferromagnetic superconductors, we analysed a model system described by a twofold orbitally degenerate Anderson lattice model. Our analysis encompassed both ferromagnetic and s-wave local inter-orbital pairing, induced by Hund's rule coupling among f-electrons. In this type of pairing, the antisymmetry of the gap function comes from its orbital part, while it is symmetric with respect to both spin and spatial components. The method of solution we used was a modified Gutzwiller approximation, within which one is able to treat also multi-band models. The justification for choosing this approximation scheme, is its relative simplicity and relevance in describing high-temperature superconductivity in strongly correlated electron systems [36], to which heavy-fermion materials also belong.

In our solutions away from the half-filling ($3 < n < 3.5$), apart from the paramagnetic phase (PM) in the regime of very strong hybridizations between f and c-electrons, we found 3 ferromagnetic phases: magnetically almost saturated FM2, half-metallic weakly saturated FM1, and a cross-over phase FM0, the latter appearing only for the case of constant density of states. Those phases have already been found in the solutions for the non-degenerate Anderson lattice model and postulated to correspond to magnetic phases clearly visible in the phase diagram of UGe_2 (Fig. 1.2). Those results have been analysed by [20, 51], assuming hybridization V being the monotonously increasing function of pressure.

Our considerations of the twofold degenerate model allowed us to supplement this picture of its magnetic and fluctuation-valence states with the mechanism of inter-orbital pairing, which could explain the superconducting phase of this material. Although our model is very simple, by e.g. containing the same degeneracy of c and f-states, only local character of the hybridization and the same microscopic parameters for both orbitals, our main task was to show that a stable mixed ferromagnetic-superconducting state is possible and how those

two orders are intertwined with each other. Thus, our most important findings are as follows.

We predict a relatively robust spin-down pairing in FM1 phase, which due to correlation effects is strongly enhanced in the vicinity of the FM2-FM1 border. It is interesting to note, that the observed critical superconducting temperature in UGe_2 is the highest precisely at this point. Nevertheless, in our solutions (except $U = 0.5$ case) the superconducting amplitude is very quickly diminishing in FM2 phase, which is actually not in accordance with the experimental results on UGe_2. Also, we predict high equal-spin pairing amplitudes in PM phase, while no superconductivity has been discovered in the paramagnetic phase of UGe_2. To sum up, while the model describes properly the principal magnetic properties of UGe_2, which has also been accomplished with its non-degenerate version [20], it does not reflect realistically the regime of stability of the superconducting phase encountered in UGe_2.

It would be very interesting to improve our $d = \infty$ results by performing the diagrammatic expansion for Gutzwiller wave-function (DE-GWF), since it is questionable whether the concrete $d = 2$ case of square lattice considered here, can be well described by the zeroth order of this expansion. As pointed out in [39], the full DE-GWF solution allows one to grasp the effective dual localized-itinerant nature of f-electrons, which is seen in experimental results for UGe_2 [52]. Also it might be useful to take into account the orbital-fluctuation effects as in [28], which may be important in stabilizing the Hund's rule induced superconductivity. Moreover, one could try to make the model more realistic, e.g by including the inter-site hybridization terms.

Appendix A

Numerical implementation

In the main part of the thesis we have found the set of equations we need to solve. Now we discuss a convenient implementation of numerical calculations. The utilised formalism is inspired by [53] and [48]. Here we also mention the numerical libraries we used in the course of producing our C++ implementation of the multi-band Gutzwiller solver.

A.1 Observables in Gutzwiller wave-function

We introduce ρ-dependent matrices M and M^c_α

$$M_{II'} \equiv \Big\langle \big|I',i\big\rangle\!\big\langle I,i\big| \Big\rangle_0 = \Big\langle \prod_{\alpha\in I}^{<} \hat{f}^\dagger_{i\alpha} \prod_{\beta\in I'}^{>} \hat{f}_{i\beta} \prod_{\gamma\notin I\cup I'} (1-\hat{n}^f_{i\gamma}) \Big\rangle_0, \tag{A.1}$$

$$[M^c_\alpha]_{II'} \equiv \Big\langle \big|I',i\big\rangle\!\big\langle I,i\big|\, \hat{c}_{i\alpha} \Big\rangle_0 = \Big\langle \prod_{\alpha\in I}^{<} \hat{f}^\dagger_{i\alpha} \prod_{\beta\in I'}^{>} \hat{f}_{i\beta} \prod_{\gamma\notin I\cup I'} (1-\hat{n}^f_{i\gamma})\, \hat{c}_{i\alpha} \Big\rangle_0. \tag{A.2}$$

Also we define constant matrices F_α, N^f_α and $\mathcal{A}^f_\sigma$

$$[F_\alpha]_{II'} \equiv \big\langle I,i\big|\hat{f}_{i\alpha}\big|I',i\big\rangle, \tag{A.3}$$

$$[N^f_\alpha]_{II'} \equiv \big\langle I,i\big|\hat{n}^f_{i\alpha}\big|I',i\big\rangle, \tag{A.4}$$

$$[\mathcal{A}^f_\sigma]_{II'} \equiv \big\langle I,i\big|\hat{f}_{i2\sigma}\hat{f}_{i1\sigma}\big|I',i\big\rangle, \tag{A.5}$$

which are matrix representations of operators $\hat{f}_{i\alpha}$, $\hat{n}^f_{i\alpha}$ and $\hat{f}_{i2\sigma}\hat{f}_{i1\sigma}$ in the local f-basis. Then the expectation values of the non-interacting part of the Hamiltonian (2.6) in which f-operators appear read

$$\begin{aligned}
\Big\langle \hat{H}^i_f \Big\rangle &= \epsilon_f \sum_\alpha \Big\langle \hat{P}_i\, \hat{n}_{i\alpha}\, \hat{P}_i \Big\rangle_0 \\
&= \epsilon_f \sum_\alpha \Big\langle \sum_{I_1I_2I_3I_4} \lambda_{I_1I_2}\, |I_1,i\rangle\langle I_2,i|\, \hat{n}_{i\alpha}\, |I_3,i\rangle\langle I_4,i|\, \lambda_{I_3I_4} \Big\rangle_0 \\
&= \epsilon_f \sum_\alpha \mathrm{Tr}\left(\lambda\cdot N^f_\alpha\cdot\lambda\cdot M\right) \qquad \text{(A.6)} \\
\Big\langle \hat{H}^i_{fc} \Big\rangle &= V \sum_\alpha \Big(\Big\langle \hat{P}_i\, \hat{f}^\dagger_{i\alpha}\, \hat{P}_i\, \hat{c}_{i\alpha} \Big\rangle_0 + \text{c.c.} \Big) \\
&= 2V \sum_\alpha \mathrm{Tr}\left(\lambda\cdot F^{\mathrm{T}}_\alpha\cdot\lambda\cdot M^c_\alpha\right), \qquad \text{(A.7)}
\end{aligned}$$

where Tr, "$\cdot$" and $(\ldots)^{\mathrm{T}}$ stand for matrix trace, multiplication and transposition respectively.

We have shown above how one calculates the occupancy of f-states and the fc hybridization amplitude. Now we also show how one can calculate the pairing amplitudes:

$$\left\langle \hat{f}_{i2\sigma}\hat{f}_{i1\sigma}\right\rangle = \mathrm{Tr}\left(\lambda\cdot\mathcal{A}^{f}\cdot\lambda\cdot M\right), \tag{A.8}$$

$$\left\langle \hat{f}_{i2\sigma}\hat{c}_{i1\sigma}\right\rangle = \mathrm{Tr}\left(\lambda\cdot F_{2\sigma}\cdot\lambda\cdot M^{c}_{1\sigma}\right). \tag{A.9}$$

Likewise, in order to calculate the expectation value of $\hat{H}_{\mathrm{int}}$ we find its matrix elements in the local f-basis

$$[E_{\mathrm{int}}]_{II'} \equiv \left\langle I,i\middle|\hat{H}_{\mathrm{int}}\middle|I',i\right\rangle, \tag{A.10}$$

such that

$$\left\langle \hat{H}_{\mathrm{int}}\right\rangle = \mathrm{Tr}\left(\lambda\cdot E_{\mathrm{int}}\cdot\lambda\cdot M\right). \tag{A.11}$$

The eigenstates and eigenvalues of matrix E_{int} are listed in Table 3.2.

Within the matrix formalism it is also straightforward to implement the constraints (3.40), (3.41), (3.32) which obtain the form

$$\mathrm{Tr}\left(\lambda\cdot\lambda\right) = 1 \tag{A.12}$$

$$\mathrm{Tr}\left(\lambda\cdot\lambda\cdot N^{f}_{1\sigma}\right) = n^{0}_{f\sigma} \tag{A.13}$$

$$\mathrm{Tr}\left(\lambda\cdot\lambda\cdot\mathcal{A}^{f}_{\sigma}\right) = A^{0}_{f\sigma} \tag{A.14}$$

All the matrix operation performed within our C++ code are done with the help of Armadillo library [54].

A.2 Integration over density of states

If the only $\mathbf{k}$-dependence comes from the dispersion of c-electrons $\epsilon_{\mathbf{k}}$, which is the case considered here, it is convenient to replace the summation over momenta $\mathbf{k}$ by the integration over the density of c-states $\mathcal{N}_c(\epsilon)$

$$\frac{1}{N}\sum_{\mathbf{k}}\mathcal{F}(\epsilon_{\mathbf{k}}) = \int d\epsilon\,\mathcal{N}_c(\epsilon)\mathcal{F}(\epsilon), \tag{A.15}$$

where $\mathcal{F}$ is any function (or matrix) depending on $\epsilon_{\mathbf{k}}$. The density of states $\mathcal{N}_c(\epsilon)$ is defined by the formula

$$\mathcal{N}_c(\epsilon) \equiv \frac{1}{N}\sum_{\mathbf{k}}\delta(\epsilon-\epsilon_{\mathbf{k}}) = \frac{1}{N}\sum_{\mathbf{k}}\lim_{s\to 0}\frac{1}{\sqrt{2\pi}s}e^{-(\epsilon-\epsilon_{\mathbf{k}})^2/2s^2}, \tag{A.16}$$

which allows for an approximate numerical evaluation of $\mathcal{N}_c(\epsilon)$ knowing $\epsilon_{\mathbf{k}}$ if we set the Gaussian width s sufficiently small.

The density of c-states which we use for the calculations in this thesis is depicted in Fig. 4.1.

A.3 Symbolic calculation of the elements of H_{eff}

Some difficulty appears in finding the actual functional dependence of the elements of H_{eff} on ρ. We approached this task by performing symbolic derivations

of the functional L using Python's library SymPy [55] and then producing out of it appropriate C++ code. However, the resulting expressions are quite lengthy and cannot be expressed as any matrix operations. A similar approach was taken to the calculation of the elements of M, M^c_α and the matrix representations of second-quantized operators: we utilized Wick's theorem in a Python script and then exported the results via SymPy to C++.

A.4 Optimization algorithm

The discussed formalism is quite useful since it explicitly introduces two classes of variational objects: matrix λ and matrices M and M^c_α, the latter depending only on ρ. It suggests the following strategy for the search of optimal solutions, in which one does not need to recalculate all the aforementioned matrices in every step:

1. start from $\lambda = \mathbb{1}$ (identity matrix), $\eta = \mathbb{0}$.
2. solve ρ-equations together with μ-equation, keeping λ constant,
3. fixing ρ and μ, solve λ- and η- equations,
4. unless the solution converged, go back to step 2.

We say solution converged, when the change of each component of the variational objects λ, η, ρ and μ in whole optimization cycle (steps 2.-3.) is not greater than some small parameter ε. After the solution converges we solve all the equations simultaneously to refine it even further.

The way we formulated the algorithm ensures that in the step 2. of the first iteration we obtain Hartree-Fock solution. The Hartree-Fock solution provides an upper bound for the ground state energy, thus if consecutive iterations lead to its higher values, we quickly know the algorithm has to be adjusted. We do it in two ways. The first one is to introduce the damping factor $x \in [0, 1]$, such that in the *i*'th iteration we start with the weighted average of (*i*-2)'th and (*i*-1)'th solutions, with weights x and $1 - x$. The other way is to randomly perturb solutions in each step, in order to avoid being trapped in a certain region of the variational space. This procedure needs to be repeated several times and among the obtained solutions the one with minimal energy is chosen.

The task we face is the solution of 18 λ-, 5 η-, 8 ρ- and 1 μ-equation, which make 32 equations in total. Although with the strategy described above we reduce the number of equations that need to be solved simultaneously, they still pose a great difficulty because of their non-linearity. There exists no deterministic method that would allow for multi-dimensional root finding in a non-linear problem. We can only resort to the methods which try to find the solutions in a neighbourhood of certain initial point. In our implementation we exploited multi-root solvers using Powell's Hybrid method from GNU Scientific Library [56], which provided us with a reasonable speed and reliability.

The typical absolute precision of our numerical results is at least 10^{-6}, which is mostly limited by the finite number of points used in the numerical integration over the density of states and the finite value of $T = 5 \cdot 10^{-5}$. We verified this by varying those quantities for certain sets of model parameters and observing the induced changes in the solutions. This accuracy is sufficient in most cases, except the case of very small superconducting condensation energies, where it was further refined.

For some ideas on the possible improvement of the implementation we refer the reader to [48, 57].

Appendix B

Renormalization factors for non-degenerate model

In case of Anderson lattice model, Gutzwiller approximation results in the renormalization of hybridization strength V. Namely,

$$V \langle \Psi_G | \hat{f}^\dagger_{i\sigma} \hat{c}_{i\sigma} | \Psi_G \rangle = \sqrt{Q_\sigma} V \langle \Psi_0 | \hat{f}^\dagger_{i\sigma} \hat{c}_{i\sigma} | \Psi_0 \rangle . \tag{B.1}$$

Here we explicitly derive renormalization factors Q_σ for the non-degenerate model, cf. (2.1), without superconductivity within Gebhard and Büenemann [29, 46] formulation of Gutzwiller approximation.

The local Hilbert space for a single f-level consists of 4 states:

$$\begin{aligned} |0\rangle &\quad (\text{unoccupied state}), \\ |\uparrow\rangle &= \hat{f}^\dagger_{i\uparrow} |0\rangle , \\ |\downarrow\rangle &= \hat{f}^\dagger_{i\downarrow} |0\rangle , \\ |\uparrow\downarrow\rangle &= \hat{f}^\dagger_{i\uparrow} \hat{f}^\dagger_{i\downarrow} |0\rangle . \end{aligned} \tag{B.2}$$

We choose the diagonal ansatz for Gutzwiller projector $\hat{P}_i$, introducing a variational parameter λ_I for each Fock state $|I\rangle$:

$$\hat{P}_i = \sum_I \lambda_I |I\rangle\langle I| , \tag{B.3}$$

where second-quantized forms of operators $|I\rangle\langle I|$ read:

$$\begin{aligned} |0\rangle\langle 0| &= \big(1 - \hat{n}^f_{i\uparrow}\big)\big(1 - \hat{n}^f_{i\downarrow}\big), \\ |\uparrow\rangle\langle\uparrow| &= \hat{n}^f_{i\uparrow}\big(1 - \hat{n}^f_{i\downarrow}\big), \\ |\downarrow\rangle\langle\downarrow| &= \big(1 - \hat{n}^f_{i\uparrow}\big)\hat{n}^f_{i\downarrow}, \\ |\uparrow\downarrow\rangle\langle\uparrow\downarrow| &= \hat{n}^f_{i\uparrow}\hat{n}^f_{i\downarrow}. \end{aligned} \tag{B.4}$$

Now we express the variational parameters λ_I in terms of physical probabilities of configurations $|I\rangle$:

$$\begin{aligned} e &\equiv \left\langle \hat{P}_i \, |0\rangle\langle 0| \, \hat{P}_i \right\rangle_0 , \\ s_\uparrow &\equiv \left\langle \hat{P}_i \, |\uparrow\rangle\langle\uparrow| \, \hat{P}_i \right\rangle_0 , \\ s_\downarrow &\equiv \left\langle \hat{P}_i \, |\downarrow\rangle\langle\downarrow| \, \hat{P}_i \right\rangle_0 , \\ d &\equiv \left\langle \hat{P}_i \, |\uparrow\downarrow\rangle\langle\uparrow\downarrow| \, \hat{P}_i \right\rangle_0 . \end{aligned} \tag{B.5}$$

This is a convenient representation of the variational space, since it leads to a transparent form of the interaction energy:

$$\langle \Psi_G | U \hat{n}^f_{i\uparrow} \hat{n}^f_{i\downarrow} | \Psi_G \rangle = Ud. \tag{B.6}$$

As one can easily verify

$$\lambda_I = \sqrt{\frac{\left\langle \hat{P}_i \, |I\rangle\langle I| \, \hat{P}_i \right\rangle_0}{\left\langle \, |I\rangle\langle I| \right\rangle_0}}. \tag{B.7}$$

Next, constraint (3.11) and two constraints (3.12) reduce the number of independent variational parameters to only one. The constraint equations

$$\left\langle \hat{P}_i^2 \right\rangle_0 = \sum_I \lambda_I^2 \left\langle \, |I\rangle\langle I| \right\rangle_0 = e + s_\uparrow + s_\downarrow + d = 1, \tag{B.8}$$

$$\left\langle \hat{P}_i^2 \hat{n}^f_{i\uparrow} \right\rangle_0 = \sum_I \lambda_I^2 \left\langle \, |I\rangle\langle I| \, \hat{n}^f_{i\uparrow} \right\rangle_0 = s_\uparrow + d = n^0_{f\uparrow}, \tag{B.9}$$

$$\left\langle \hat{P}_i^2 \hat{n}^f_{i\downarrow} \right\rangle_0 = \sum_I \lambda_I^2 \left\langle \, |I\rangle\langle I| \, \hat{n}^f_{i\downarrow} \right\rangle_0 = s_\downarrow + d = n^0_{f\downarrow}, \tag{B.10}$$

where

$$n^0_{f\sigma} \equiv \left\langle \hat{n}^f_{i\sigma} \right\rangle_0 , \tag{B.11}$$

determine unequivocally parameters e, $s_\uparrow$ and $s_\downarrow$ in terms of d. Note that because $\hat{P}_i$ commutes with $\hat{n}^f_{i\sigma}$, equations (B.9) and (B.10) imply the equality of particle number in the correlated $|\Psi_G\rangle$ and non-correlated state $|\Psi_0\rangle$:

$$\langle \Psi_G | \hat{n}^f_{i\sigma} | \Psi_G \rangle = \langle \Psi_0 | \hat{n}^f_{i\sigma} | \Psi_0 \rangle . \tag{B.12}$$

Finally, we calculate the fc hybridization amplitude in the correlated state $|\Psi_G\rangle$

$$\begin{aligned} \left\langle \hat{P}_i f^\dagger_{i\sigma} c_{i\sigma} \hat{P}_i \right\rangle_0 &= \sum_{II'} \lambda_I \lambda_{I'} \left\langle |I\rangle\langle I| \, f^\dagger_{i\sigma} \, |I'\rangle\langle I'| \, c_{i\sigma} \right\rangle_0 \\ &= \frac{\sqrt{s_\sigma e} + \sqrt{d s_{\bar{\sigma}}}}{\sqrt{n^0_{f\sigma}(1 - n^0_{f\sigma})}} \left\langle f^\dagger_{i\sigma} c_{i\sigma} \right\rangle_0 \end{aligned} \tag{B.13}$$

and express the renormalization factor Q_σ solely in terms of d and $n^0_{f\sigma}$

$$Q_\sigma = \frac{\left(\sqrt{(n^0_{f\sigma}-d)(1-n^0_{f\uparrow}-n^0_{f\downarrow}+d)}+\sqrt{d\,(n^0_{f\bar{\sigma}}-d)}\right)^2}{n^0_{f\sigma}(1-n^0_{f\sigma})}. \tag{B.14}$$

Additionally, one can check by explicit calculation that only due to (B.9) and (B.10) the following relations hold

$$\left\langle \hat{P}_i^2 \hat{n}^c_{i\sigma} \right\rangle_0 = \left\langle \hat{P}_i \hat{n}^c_{i\sigma} \hat{P}_i \right\rangle_0 = \left\langle \hat{n}^c_{i\sigma} \right\rangle_0, \tag{B.15}$$

$$\left\langle \hat{P}_i^2 \hat{f}^\dagger_{i\sigma} \hat{c}_{i\sigma} \right\rangle_0 = \left\langle \hat{f}^\dagger_{i\sigma} \hat{c}_{i\sigma} \right\rangle_0. \tag{B.16}$$

Bibliography

[1] S. S. Saxena et al., "Superconductivity on the border of itinerant-electron ferromagnetism in UGe_2", Nature **406**, 587–592 (2000).

[2] D. Aoki et al., "Coexistence of superconductivity and ferromagnetism in URhGe", Nature **413**, 613–616 (2001).

[3] N. T. Huy et al., "Superconductivity on the Border of Weak Itinerant Ferromagnetism in UCoGe", Phys. Rev. Lett. **99**, 067006 (2007).

[4] C. Pfleiderer, "Superconducting phases of f -electron compounds", Rev. Mod. Phys. **81**, 1551–1624 (2009).

[5] A. D. Huxley, "Ferromagnetic superconductors", Physica C **514**, 368 (2015).

[6] M. B. Maple and Ø. Fischer, *Superconductivity in Ternary Compounds II* (Springer US, 1982).

[7] K. Machida and T. Ohmi, "Phenomenological Theory of Ferromagnetic Superconductivity", Phys. Rev. Lett. **86**, 850 (2001).

[8] D. Fay and J. Appel, "Coexistence of *p*-state superconductivity and itinerant ferromagnetism", Phys. Rev. B **22**, 3173 (1980).

[9] T. R. Kirkpatrick et al., "Strong Enhancement of Superconducting T_c in Ferromagnetic Phases", Phys. Rev. Lett. **87**, 127003 (2001).

[10] K. G. Sandeman, G. G. Lonzarich, and A. J. Schofield, "Ferromagnetic Superconductivity Driven by Changing Fermi Surface Topology", Phys. Rev. Lett. **90**, 167005 (2003).

[11] J. Linder et al., "Coexistence of itinerant ferromagnetism and a nonunitary superconducting state with line nodes: Possible application to UGe_2", Phys. Rev. B **77**, 184511 (2008).

[12] A. Klejnberg and J. Spałek, "Hund's rule coupling as the microscopic origin of the spin-triplet pairing in a correlated and degenerate band system", J. Phys. Condens. Matter **11**, 6553 (1999).

[13] A. Klejnberg and J. Spałek, "Metal-insulator transition, gap opening due to the combined orbital-spin ordering, and spin-triplet superconductivity", Phys. Rev. B **61**, 15542–15545 (2000).

[14] J. Spałek, "Spin-triplet superconducting pairing due to local Hund's rule and Dirac exchange", Phys. Rev. B **63**, 104513 (2001).

[15] M. Zegrodnik and J. Spałek, "Coexistence of spin-triplet superconductivity with magnetic ordering in an orbitally degenerate system: Hartree-Fock-BCS approximation revisited", Phys. Rev. B **86**, 014505 (2012).

[16] M. Zegrodnik, J. Spałek, and J. Bünemann, "Coexistence of spin-triplet superconductivity with magnetism within a single mechanism for orbitally degenerate correlated electrons: statistically consistent Gutzwiller approximation", New J. Phys. **15**, 073050 (2013).

[17] J Spałek and M Zegrodnik, "Spin-triplet paired state induced by Hund's rule coupling and correlations: a fully statistically consistent Gutzwiller approach", J. Phys. Condens. Matter **25**, 435601 (2013).

[18] M. Zegrodnik, J. Spałek, and J. Bünemann, "Even-parity spin-triplet pairing by purely repulsive interactions for orbitally degenerate correlated fermions", New J. Phys. **16**, 033001 (2014).

[19] M. Zegrodnik, "Even-parity spin-triplet paired states by combined effect of Hund's rule and correlations in two-band Hubbard model: a brief overview", Philos. Mag. **95**, 574–582 (2014).

[20] M. M. Wysokiński, M. Abram, and J. Spałek, "Ferromagnetism in UGe_2: A microscopic model", Phys. Rev. B **90**, 081114(R) (2014).

[21] M. M. Wysokiński, M. Abram, and J. Spałek, "Criticalities in the itinerant ferromagnet UGe_2", Phys. Rev. B **91**, 081108(R) (2015).

[22] M. Abram, M. M. Wysokiński, and J. Spałek, "Tricritical wings in UGe_2: A microscopic interpretation", J. Magn. Magn. Mater. **400**, 27–30 (2016).

[23] C. Pfleiderer and A. D. Huxley, "Pressure Dependence of the Magnetization in the Ferromagnetic Superconductor UGe_2", Phys. Rev. Lett. **89**, 147005 (2002).

[24] A. B. Shick and W. E. Pickett, "Magnetism, Spin-Orbit Coupling, and Superconducting Pairing in UGe_2", Phys. Rev. Lett. **86**, 300–303 (2001).

[25] K. Oikawa et al., "Crystal Structure of UGe_2", J. Phys. Soc. Jpn. **65**, 3229–3232 (1996).

[26] A. V. Chubukov, D. Pines, and J. Schmalian, "A Spin Fluctuation Model for *d*-Wave Superconductivity", in *The physics of superconductors*, edited by K. H. Bennemann and J. B. Ketterson (Springer Berlin Heidelberg, Berlin, Heidelberg, 2003), 495–590.

[27] D. J. Scalapino, "A common thread: The pairing interaction for unconventional superconductors", Rev. Mod. Phys. **84**, 1383–1417 (2012).

[28] S. Hoshino and P. Werner, "Superconductivity from Emerging Magnetic Moments", Phys. Rev. Lett. **115**, 247001 (2015).

[29] J. Bünemann, W. Weber, and F. Gebhard, "Multiband Gutzwiller wave functions for general on-site interactions", Phys. Rev. B **57**, 6896 (1998).

[30] M. C. Gutzwiller, "Effect of Correlation on the Ferromagnetism of Transition Metals", Phys. Rev. Lett. **10**, 159 (1963).

[31] D. Vollhardt, "Normal ^{3}He: an almost localized Fermi liquid", Rev. Mod. Phys. **56**, 99–120 (1984).

[32] T. M. Rice and K. Ueda, "Gutzwiller Variational Approximation to the Heavy-Fermion Ground State of the Periodic Anderson Model", Phys. Rev. Lett. **55**, 995–998 (1985).

[33] P. Fazekas and B. H. Brandow, "Application of the Gutzwiller method to the periodic Anderson model", Phys. Scr. **36**, 809–819 (1987).

[34] J. Jędrak and J. Spałek, "Consistent statistical treatment of the renormalized mean field *t-J* model", Phys. Rev. B **81**, 073108 (2010).

[35] J. Jędrak, J. Kaczmarczyk, and J. Spałek, *Statistically-consistent Gutzwiller approach and its equivalence with the mean-field slave-boson method for correlated systems*, arXiv:1008.0021 [cond-mat.str-el] (2010).

[36] J. Spałek, M. Zegrodnik, and J. Kaczmarczyk, "Universal properties of high temperature superconductors from real space pairing: quantitative comparison with experiment", arXiv:1606.03247 [cond-mat.supr-con], submitted to Sci. Rep. (2016).

[37] J. Bünemann, T. Schickling, and F. Gebhard, "Variational study of Fermi surface deformations in Hubbard models", EPL **98**, 27006 (2012).

[38] J. Kaczmarczyk et al., "Superconductivity in the two-dimensional Hubbard model: Gutzwiller wave function solution", Physical Review B **88**, 115127 (2013).

[39] M. M. Wysokiński, J. Kaczmarczyk, and J. Spałek, "Gutzwiller wave-function solution for Anderson lattice model: Emerging universal regimes of heavy quasiparticle states", Physical Review B **92**, 125135 (2015).

[40] M. M. Wysokiński, J. Kaczmarczyk, and J. Spałek, "Correlation-driven d-wave superconductivity in Anderson lattice model", arXiv:1510.00224 [cond-mat.str-el], accepted to Phys. Rev. B (2016).

[41] Z. Fisk et al., "Heavy-electron metals", Nature **320**, 124–129 (1986).

[42] H. Tsunetsugu, M. Sigrist, and K. Ueda, "The ground-state phase diagram of the one-dimensional Kondo lattice model", Rev. Mod. Phys. **69**, 809–864 (1997).

[43] J. Kanamori, "Electron Correlation and Ferromagnetism of Transition Metals", Prog. Theor. Phys. **30**, 275 (1963).

[44] P. Nozières and S. Schmitt-Rink, "Bose condensation in an attractive fermion gas: From weak to strong coupling superconductivity", J. Low Temp. Phys. **59**, 195 (1985).

[45] A. J. Leggett, *Quantum liquids Bose condensation and Cooper pairing in condensed-matter systems* (Oxford University Press, 2006).

[46] F. Gebhard, "Gutzwiller correlated wave functions in finite dimensions d : A systematic expansion in $1/\ d$", Phys. Rev. B **41**, 9452 (1990).

[47] J. Bünemann et al., "Gutzwiller-Correlated Wave Functions: Application to Ferromagnetic Nickel", in *Frontiers in magnetic materials*, edited by A. V. Narlikar (Springer Berlin Heidelberg, Berlin, Heidelberg, 2005), pp. 117–151.

[48] J. Bünemann et al., "Numerical minimisation of Gutzwiller energy functionals", Phys. Status Solidi B **249**, 1282 (2012).

[49] W. Metzner and D. Vollhardt, "Correlated Lattice Fermions in d=∞ Dimensions", Phys. Rev. Lett. **62**, 324 (1989).

[50] J. Bünemann, F. Gebhard, and R. Thul, "Landau-Gutzwiller quasiparticles", Phys. Rev. B **67**, 075103 (2003).

[51] K. Kubo, "Ferromagnetism and Fermi surface transition in the periodic Anderson model: Second-order phase transition without symmetry breaking", Phys. Rev. B **87**, 195127 (2013).

[52] R. Troć, Z. Gajek, and A. Pikul, "Dualism of the 5f electrons of the ferromagnetic superconductor UGe_2 as seen in magnetic, transport, and specific-heat data", Phys. Rev. B **86**, 224403 (2012).

[53] M. Fabrizio, "Gutzwiller description of non-magnetic Mott insulators: Dimer lattice model", Phys. Rev. B **76**, 165110 (2007).

[54] C. Sanderson and R. Curtin, "Armadillo: A template-based C++ library for linear algebra", Journal of Open Source Software **1**, 26 (2016).

[55] SymPy Development Team, *SymPy: Python library for symbolic mathematics*, `http://www.sympy.org` (2016).

[56] M. Galassi et al., *GNU Scientific Library Reference Manual - Third Edition* (Network Theory Ltd., 2009).

[57] J. Kaczmarczyk, T. Schickling, and J. Bünemann, "Evaluation techniques for Gutzwiller wave functions in finite dimensions", Phys. Status Solidi B **252**, 2059–2071 (2015).